Discovery of Novel Effector Protein Candidates Produced in the Dorsal Gland of **Root-Knot Nematode Adult Females** Raquel O. Rocha<sup>1</sup>, Richard S. Hussey<sup>1</sup>, Lauren E. Pepi<sup>2</sup>, Parastoo Azadi<sup>2</sup>, Melissa G. Mitchum<sup>1\*</sup> <sup>1</sup>Department of Plant Pathology and Institute of Plant Breeding, Genetics, and Genomics, University of Georgia, Athens, GA 30602, U.S.A. <sup>2</sup>Complex Carbohydrate Research Center, University of Georgia, Athens, GA 30602, U.S.A. \*Corresponding author: Melissa G. Mitchum; melissa.mitchum@uga.edu Keywords: adult females, effectors, dorsal gland, Meloidogyne, nematode Funding: University of Georgia Office of the President and Georgia Agricultural Experiment Stations to MGM; US National Institutes of Health (R24GM137782 to PA); GlycoMIP, a National Science Foundation Materials Innovation Platform funded through Cooperative Agreement DMR-1933525. 

### ABSTRACT (235 words)

24

25

26

27

28

29

30

31

32

33

34

35

36

37

38

39

40

41

42

43

44

45

Root-knot nematodes (RKN; *Meloidogyne* spp.) represent one of the most damaging groups of plant-parasitic nematodes. They secrete effector proteins through a protrusible stylet to manipulate host cells for their benefit. Stylet-secreted effector proteins are produced within specialized secretory esophageal gland cells, one dorsal (DG) and two subventral (SvG), whose activity differ throughout the nematode life cycle. Previous gland transcriptomic profiling studies identified dozens of candidate RKN effectors, but were focused on the juvenile stages of the nematode when the SvGs are most active. We developed a new approach to enrich for the active DGs of RKN M. incognita adult females for RNA and protein extraction. Female heads were manually cut from the body, and a combination of sonication/vortexing was used to dislodge contents inside the heads. DG-enriched fractions were collected by filtering using cell strainers. Comparative transcriptome profiling of pre-parasitic second-stage juveniles, female heads, and DG-enriched samples was conducted using RNA sequencing. Application of an established effector mining pipeline led to the identification of 83 candidate effector genes upregulated in DG-enriched samples of adult females that code for proteins with a predicted signal peptide, but lack transmembrane domains or homology to proteins in the free-living nematode Caenorhabditis elegans. In situ hybridization resulted in the identification of 14 new DG-specific candidate effectors expressed in adult females. Taken together, we have identified novel candidate Meloidogyne effector genes that may have essential roles during later stages of parasitism.

48

49

50

51

52

53

54

55

56

57

58

59

60

61

62

63

64

65

66

67

68

69

### INTRODUCTION

Root-knot nematodes (RKN), *Meloidogyne* spp., represent one of the most significant groups of plant-parasitic nematodes (PPN), limiting the agricultural industry from meeting the increasing demands for food, feed, fuel, and fiber (Jones et al., 2013). Members of this genus have a world-wide distribution and are capable of infecting a wide range of cultivated crop plant species (Chitwood, 2003). Known for their ability to induce large galls, or "knots", on their host root system, these nematodes secrete proteins through a hollow, protrusible stylet to first mechanically penetrate and migrate through the roots and later induce a feeding site comprised of 5-7 giant cells (GCs) within the vascular cylinder. The GCs transcriptional, metabolic, and cellular processes are re-programmed to supply nutrients for the developing nematode. These cells expand hundreds of times the size of a normal root cell while undergoing repeated rounds of karyokinesis uncoupled from cytokinesis to become multinucleate, with large, lobe-shaped nuclei; and simultaneously increase the cytoplasm density and the abundance of ribosomes, endoplasmic reticulum, mitochondria, and Golgi bodies. (Escobar et al., 2015; Mitchum et al., 2013). As GCs enlarge, central vacuoles are fragmented into small ones, cell wall ingrowths form, and starch accumulation in chloroplast-like structures is induced (Ji et al., 2013; Jones and Gotto, 2011). Once a feeding site is established, the juveniles undergo molting and growth until they develop into swollen sedentary adult females. Females for most *Meloidogyne* species will parthenogenically produce hundreds of eggs deposited in a gelatinous matrix on the root surface, thus re-initiating the life cycle (Goode and Mitchum 2022).

These critical events in the RKN life cycle are mediated by the production and secretion of effector proteins. Stylet-secreted effector proteins are produced by highly specialized secretory esophageal gland cells, one dorsal (DG) and two subventral (SvG), differing in their role according to the life stage of the nematode (Davis et al., 2008; Hussey, 1989; Mitchum et al., 2013; Vieira and Gleason, 2019). During early parasitism, when the nematode is still motile, the SvGs are larger and more active than the DG cell, producing cell-wall digesting enzymes and a suite of effectors to suppress plant immunity that are used by the second-stage juveniles to gain access to host root cells (Hussey et al., 2002; Wang et al., 2018; Qin et al., 2022). Once the nematode becomes sedentary, the single DG gland cell is then stimulated to become the primary source of secretions related to the formation and maintenance of the GCs, which serve as the sole nutrient source for the nematode. Because of the wide range of cellular events a RKN needs to coordinate and exploit without triggering any defense responses from the host, the arsenal of effectors this pathogen requires is equally diverse. Thus, a community-wide effort has been made to elucidate the secretome of RKN esophageal gland cells for identifying effectors involved in nematode parasitism. To identify stylet-secreted effectors, researchers have focused on developing methods to isolate and analyze intact nematode gland cells or their contents for molecular studies that has led to a diverse catalogue of candidates for functional studies (Espada et al., 2018; Gao et al., 2001; Maier et al., 2013, 2021; Mitchum et al., 2023; Rutter et al., 2014; Vieira et al., 2020). However, current knowledge in effector discovery and characterization mostly focuses on early events in

70

71

72

73

74

75

76

77

78

79

80

81

82

83

84

85

86

87

88

89

90

91

92

the RKN life cycle, mainly when SvG gland cells are still mostly active (Ding et al., 1998; Ding et al., 2000; Jaubert et al., 2002; Lambert et al., 1999; Leelarasamee et al., 2018; Mejias et al., 2021; Qin et al., 2022). Relatively little is known about the profile of DG effectors at later stages of parasitism and how they function in the maintenance of GCs.

Here, we set out to identify new effector candidates predominantly expressed in DG during the late stages of the RKN life cycle, specifically in the sessile, but actively feeding, adult females. For this, a new approach was used to enrich for DG cells from adult females for transcriptomic and proteomic analysis. We identified 83 DG effector gene candidates coding for mostly (96%) novel predicted secreted proteins with no associated functional annotation. Of these, 19 were previously shown to be expressed within RKN esophageal gland cells, validating our approach. Twenty-seven of the 63 newly discovered DG effector gene candidates were selected for in situ hybridization and 14 (52%) of these were confirmed to be specifically expressed in the DG cell of adult RKN females.

#### RESULTS

# Development and validation of an adult female DG enrichment method

A transcriptomic panel of effector candidates during late RKN parasitism was developed using a protocol to enrich the highly active DGs of *M. incognita* adult females without the labor-intensive and time-consuming approaches of micro-manipulating the glands for isolation or micro-aspirating the gland cytoplasm (Hussey et al., 2011; Maier et al.,

2013). Instead, a combination of manual cutting of adult female heads with sonication, vortexing, and cell strainer filtration was used to enrich samples for DG cells.

From the vortexed/sonicated homogenates of 50 female heads, approximately 20% of the DGs were separated entirely from the nematode heads and dissociated from the cuticle and most of the nematode tissue (**Figure 1a**). Because most detached DGs measured  $80-90~\mu m$  in length and 25-30  $\mu m$  in width, samples were sequentially filtered through two cell strainers of  $70~\mu m$  and  $10~\mu m$  mesh size, respectively. DGs were retained on the  $10~\mu m$  strainer, but were not entirely free of other nematode organs within the filters mesh dimensions (e.g., metacorpus, SvG).

To confirm the enrichment of DGs in the samples, we quantified transcript levels of three candidate effector genes previously shown to be expressed exclusively within the DG of young adult females, using quantitative reverse-transcription PCR (qRT-PCR). Transcript abundance of the DG secretory proteins 1 (*msp1* or *2E07*), 6 (*msp6* or *7A01*), and 12 (*msp12* or *11A01*) (Huang et al., 2003) showed a relative expression enrichment of 45, 54, and 47 times when compared to *M. incognita* whole adult females (WF), respectively (**Figure 1b-c**), while the second-stage pre-parasitic juvenile (ppJ2) samples did not show expression of these genes. When compared to female heads (FH), *msp1*, *msp6*, and *msp12* relative transcript abundances were at least five times higher in DG samples, thus confirming the utility of the method to enrich for DGs from RKN adult females for transcriptomic studies.

## Sequencing and assembly of life stage-specific transcriptomes

RNA sequencing of three samples, including ppJ2, FH, and DG-enriched samples, was carried out (**Figure 2a**). Following the initial passing filter, RNA sequencing using the Illumina platform generated a total of 720,441,122 paired-end 50 base reads, with 87.39% of the bases at or above a quality score of 30. Further quality trimming retained only paired-end reads with a minimum length of 30 bases for downstream mapping. This resulted in an average of 17,498,855 trimmed reads per sample, which still granted ample coverage for this RNA-seq analysis. When mapped to the *M. incognita* v3 reference genome (Blanc-Mathieu et al., 2017), an average of 10,251,612 reads, corresponding to 58.59% of the reads from all samples, were uniquely mapped. Overall, 37,160 unique genes of the 43,718 coding genes in the genome were identified across the three experimental samples. Hierarchical clustering analysis of the rlog-transformed expression data based on Manhattan's rank coefficient showed the three experimental groups clustered well together with a higher correlation between FH and DG-enriched sample groups, with ppJ2 as a distinct outlier (**Supplementary figure 1**).

# Prediction of candidate effectors in the DG-enriched transcriptome

We next conducted pairwise comparisons among the three experimental groups to identify differentially expressed genes (DEGs). To distinguish effector gene candidates from housekeeping genes and to identify those that might have a more active role in parasitism during the adult female life stage, we restricted our analysis to genes upregulated in DG-enriched samples of adult females in comparison to ppJ2s that had not yet infected host roots. We also reasoned that an upregulation of genes in DG-enriched samples in comparison to FH heads would filter out candidates that are more

likely to be expressed within DGs as opposed to other cells present in the adult female head.

Pairwise comparisons of genes expressed in DG-enriched samples with those expressed in ppJ2 and FH identified 8,468 and 1,688 upregulated genes in DG, respectively. Potential DG effector candidates were thus considered to be present within the 461 genes with increased expression levels in DG samples common in both comparisons (DG-enriched vs. ppJ2 and DG-enriched vs. FH) (**Figure 2b**). Three of these were determined to be non-coding RNA and thus were not carried over to the subsequent analysis steps.

An analysis using the SignalP program (Almagro et al., 2019) refined our list to 120 genes encoding proteins containing a predicted N-terminal signal peptide and lacking transmembrane domains, which suggests their product may be targeted for secretion from the nematode stylet for parasitizing host cells. Although there are reported examples of housekeeping genes neofunctionalizing to a role in plant parasitism (e.g., glutathione synthetase described by Lilley et al., 2018), we chose to explore effector candidates not sharing homologs in non-parasitic nematode species. Therefore, we removed any predicted secreted proteins from our analysis that shared homology to proteins found in the free-living nematode *C. elegans*. This resulted in a final list of 83 DG effector gene candidates (**Figure 2c, Supplementary table 1**). Further cross-referencing of the 83 predicted DG effector protein candidates to a list of *M. incognita* proteins specific to PPN (Danchin, 2020; available at <a href="https://doi.org/10.15454/19MWRS">https://doi.org/10.15454/19MWRS</a>)

identified 81 to be PPN-specific. However, a BLASTp search using the protein sequences of Minc3s00144g05949 and Minc3s01699g25716, the two genes not classified as PPN-specific according to Danchin (2020), found similarities only against PPN species. Five out of the 83 genes (Minc3s05190g37766, Minc3s05895g38985, Minc3s01550g24644, Minc3s00371g11166, and Minc3s01699g25716) have similarity to proteins in *Heterodera glycines*. Of the 83 predicted DG effector protein candidates, 80 candidates had no associated functional annotation and 19 were either previously shown to be expressed in RKN esophageal gland cells or shared >70% similarity to a gene previously shown to be expressed in RKN esophageal gland cells (Huang et al., 2003; Nguyen et al., 2018; Rutter et al., 2014). The remaining 64 *Mincs* represented newly discovered DG effector gene candidates expressed in adult females.

The increasing number of transcriptomic studies has advanced the identification of the PPN effector repertoire to identify new effector-like properties. Among all groups of plant pathogens, a significant number of effector proteins are targeted to the host plant cell nucleus (Rivas and Genin, 2011). In this context, *in silico* analysis using NLStradamus (Nguyen et al., 2009) identified 24 genes encoding secreted proteins with a predicted nuclear localization signal (NLS). We also identified a set of 36 genes containing a putative cis-regulatory promoter element previously found to be associated with *Meloidogyne* DG effectors (Mel-DOG box) (Da Rocha et al., 2021). Finally, 68 (82%) of our DG effector candidates harbored an effector-enriched motif (MERCI motif) in the 100 first amino acids (Grynberg et al., 2020; Vens et al., 2011) (**Figure 2d**, **Supplementary table 1**).

209

210

211

212

213

214

215

216

217

218

219

220

221

222

223

224

225

226

227

228

229

230

# *In situ* hybridization

In situ hybridization analysis was carried out for 27 of the 64 newly discovered effector gene candidates to determine their tissue-specific expression pattern within female heads. The control gene, Minc3s00173q06738 (or 2E07; identified by Huang et al., 2003), previously shown to be expressed within the DG cell of earlier parasitic stages, remained highly expressed in the DG of adult females (Figure 3a). We further confirmed the expression of 14 newly discovered candidate effectors exclusively within the DG of adult females (Table 1; Figure 3a). Of these, four of the Minc genes confirmed to be DG-expressed shared at least 70% nucleotide similarity with other genes within our 83 effector candidate list; therefore, we cannot rule out cross-reaction of the used probes across genes of the same family. In addition, Minc3s00371g11166 (or Minc08073; Rutter et al., 2014), was previously described as SvG-expressed, but here we determined it to be DG-expressed in our analysis of adult females (Figure 3a). Two Mincs, Minc3s01802g26418 (or 8H11; identified by Huang et al., 2003) and Minc3s05190g37766 (homolog to 30H07; identified by Huang et al., 2003), both on the list of 83 DG effector gene candidates, but previously shown to be expressed in the SvG of earlier parasitic stages, were found to still be actively expressed in the SvG of adult females (Figure 3b). One newly identified DG effector gene candidate tested, Minc3s00180g06933, was also expressed in the SvG (Figure 3b). These results suggest that SvG glands may still retain some activity in adult females and were captured at some level along with adult females DGs using our enrichment protocol.

232

233

234

235

236

237

238

239

240

241

242

243

244

245

246

247

248

249

250

251

252

253

From the remaining tested genes, two candidates were confirmed to be expressed within the female metacorpus, five candidates showed diffuse expression that could not be assigned to a specific organ, and seven candidates showed no signal of hybridization either due to low expression or non-optimal probe design (Supplementary figure 2). Integrative transcriptome and proteome analysis of DG-enriched samples A glycoproteomics approach was also conducted in parallel on a DG-enriched sample. A total of 10,910 unique proteins were identified following LC-MS/MS with no data filter. Out of those, 4,205 unique proteins had Byonic scores greater than 50 and over 5% of the protein sequence covered by peptide-spectrum matches (Bern et al., 2012). Glycosylation was detected in 2,074 non-filtered proteins, with most of the identified glycopeptides containing high mannose glycoforms. *Minc* genes corresponding to 9,121 proteins detected by this method were also present in DG-enriched samples subjected to RNA sequencing (Supplementary figure 3a). Further analysis revealed 404 proteins with a predicted SP, no TMM, and lacking any homology to proteins found in *C. elegans* (Supplementary figure 3b). Out of these, 342 proteins were specific to PPN, 317 had a predicted MERCI effector motif, and 87 contained a nuclear localization signal (NLS). The *Minc* genes corresponding to 71 proteins had a Mel-DOG box promoter motif (Supplementary figure 3c). When cross compared to the DG effector candidate shortlist from transcriptomic analysis, 28 genes in common were identified (Supplementary figure 3d, Supplementary table 2).

DISCUSSION

Most RKN effectors discovered to date are expressed during the early stages of infection and parasitism, with roles in penetration, migration, host defense suppression, and the initiation of feeding cells (Ding et al., 1998; Ding et al., 2000; Jaubert et al., 2002; Lambert et al., 1999; Leelarasamee et al., 2018; Mejias et al., 2021; Qin et al., 2022). Much less is known about the effectors actively secreted by adult females to modulate the late stages of plant-nematode interactions following feeding site establishment. Prior studies have demonstrated robust DG activity and reduced SvG activity in adult females (Davis et al., 2004; Huang et al., 2003); however, effector proteins with roles in sustained giant cell function and nematode feeding remain to be discovered.

To address this gap in knowledge and identify effector candidates expressed during late stages of RKN parasitism, we developed a protocol to enrich for DG cells of adult females. The combined manual cutting of female heads with sonication and vortexing to dislodge the contents inside the heads coupled with filtering using cell strainers, enriched samples for DGs. DG enrichment was validated by a demonstrated increase in transcript abundance of three known DG-expressed genes over 40 times in comparison to whole adult females. Despite contamination with nematode organs of similar DG size (i.e., metacorpus) and an inability to completely detach all SvG cells, the method developed here was advantageous, as a simpler, more straightforward, and faster approach than micro-manipulation or micro-aspiration of the glands (Hussey et al.,

278

279

2011; Maier et al., 2013). Taking into consideration the potential differences in sizes of SvG and DG cells across PPN species, this method is adaptable to enrich esophageal gland cells from different life stages of other nematode species by adjusting the mesh size of the cell strainer.

281

282

283

284

285

286

287

288

289

290

291

292

293

294

295

296

280

The resulting DG-enriched transcriptome consisted of over 33,000 transcripts. To prioritize potential effectors expressed in the DG of adult females, we identified common upregulated genes in pairwise comparisons of DG-enriched samples with either ppJ2 or FHs. Our interest was in capturing *Minc* genes highly active in DGs of adult females and thus, with functions more likely related to the maintenance of feeding cells and nematode feeding. Therefore, we applied a stringent analysis pipeline that excluded DG-expressed genes in juvenile stages unless they were upregulated in DG-enriched samples in comparison to ppJ2. Our effector mining strategy was similar to what has been performed by other groups by selecting effector candidates carrying predicted Nterminal signal peptides within their protein sequences, lacking transmembrane domains, and sharing no homology to the free-living nematode C. elegans (Da Rocha et al., 2020; Grynberg et al., 2020; Huang et al., 2003; Rutter et al., 2014). This strategy identified 83 putative DG effector gene candidates, including 10 genes, with nine homolog genes sharing high protein sequence similarity, to previously identified effector gene candidates expressed in DG cells of earlier life stages.

297

298

299

Only 27 genes carried any associated Gene Ontology description, the most common one, for 14 of the genes, being an integral component on the membrane, despite their

lack of a TMM predicted by SignalP. With little functional annotation information available, we then categorized our list of 83 DG effector gene candidates according to multiple effector-related features, including genes having a Mel-DOG box promoter motif (36 candidates) (Da Rocha et al., 2021), and predicted SP-positive proteins containing a nuclear localization signal (24 candidates), or a predicted MERCI effector motif (68 candidates). Only seven genes in this list did not encode a protein with a recognized RKN effector-related motif. Out of these seven genes, two (Minc3s05136g37655 and Minc3s07416g41097) were previously described by Nguyen et al. (2018) as candidate secreted effectors, one (Minc3s00689g16113) was confirmed here as a metacorpus-expressed gene by *in situ* hybridization, and one (Minc3s00007g00501) showed no signal of hybridization (data not shown).

We also classified the 83 DG effector gene candidates according to hierarchical clusters based on their expression profiles across all life stages (Da Rocha et al. 2021). While representatives of all eight clusters were observed, most of the genes (37) were grouped into clusters G and H, which comprised genes that peaked in expression during the parasitic third- and fourth-stage juveniles (J3/J4), during which the nematode does not have a stylet and does not feed. Da Rocha and collaborators (2021) determined SvG and DG effectors were enriched in clusters C, G, and H. Consistent with this, 50% of our effector candidates were distributed across these same three clusters. Nevertheless, 37% of genes in our list were not classified into any cluster because they were not identified by Da Rocha et al., (2021) as differentially expressed

genes between the four life stages examined (ppJ2s, a mix of parasitic J3/J4, adult females, and eggs).

324

325

326

327

328

329

330

331

332

333

334

335

336

337

338

339

340

341

342

322

323

We also selected a subset of the newly identified DG effector candidate genes for in situ hybridization to determine if these genes were indeed expressed in the DG of adult females. Of the 27 tested, we identified 14 DG effector candidate genes that were expressed exclusively within the DG cell of adult females. One newly identified DG effector candidate gene (Minc3s00180g06933) present in our 83 DG effector gene candidate list was found to be expressed within the SvG consistent with the expression pattern observed for SvG-expressed controls (8H11 and Minc3s05190g37766), also present in our 83 effector gene candidate list, indicating some level of activity of these cells during the late stages of parasitism. Surprisingly, both SvG-expressed controls did not have a Mel-DOG box promoter motif, however, the newly discovered SvGexpressed Minc gene Minc3s00180g06933 did. Of the genes tested by in situ hybridization and confirmed to be DG-expressed, all but five had a Mel-DOG box promoter motif. According to Da Rocha et al., (2021), the Mel-DOG box is a putative seven-nucleotide cis-regulatory motif associated with effector candidates expressed within DGs and conserved across the clade I of root-knot nematodes. Although the presence of a Mel-DOG box in the promoter region of a gene is a significant criterion to predict new DG effector candidates in silico, our analysis shows that, it is not a requirement for DG expression nor is it exclusive to DG expression.

343

We also explored the possibility of adapting the DG-enrichment technique for proteomic/glycoproteomic analysis. The multi-layer regulation of proteins is dependent not just on transcript abundance but also determined by mRNA processing, translation, and protein turnover levels (Zapalska-Sozoniuk et al., 2019). Thus, identifying the proteome profile of DG-enriched samples has the potential to uncover effector candidates that have a poor correlation between mRNA-protein ratios and thus could not be identified by a transcriptomic approach alone. In addition, glycosylation is a post-translational modification essential for biological function, but not coded in DNA or RNA sequences (Wang et al., 2014). Protein glycosylation, the covalent attachment of complex carbohydrates to specific amino acids within the protein sequence, is one of the most common protein modifications among the over 400 types described in cells and has a significant role in mediating host-pathogen interactions (Bagdonaite et al., 2022; Lin et al., 2020; Ramazi and Zahiri, 2021).

In our exploratory glycoproteomic analysis, a total of 10,910 proteins were identified in the DG-enriched sample with no data filters. Nineteen percent were detected as glycosylated. Most of the glycopeptides identified contained high-mannose glycoforms, the most abundant class of N-glycosylation in nematode biological samples (Paschingeret al., 2019; Wang et al., 2021). Of the 10,910 proteins, 1,005 (9.21%) contained a predicted SP. Filtering of the predicted secreted proteins to remove those sharing any homology to *C. elegans* and categorizing the remaining ones according to the effector-related features mentioned earlier (DOG box promoter motif, MERCI motif, nuclear localization signal) resulted in 404 DG effector candidates obtained from our

368

369

370

371

372

373

374

375

376

377

378

379

380

381

382

383

384

proteomics approach, with 176 of these having Byonic scores greater than 50 and over 5% of the protein sequence covered. Byonic scores indicate the absolute quality of the best peptide-spectrum match for the identified protein (Bern et al., 2012). This criterion, combined to the percentage of the protein sequence covered by the identified peptides, increases the confidence of protein identification. Twenty-eight effector candidates identified by LC-MS/MS were in common with our 83 DG effector candidate gene shortlist identified by RNA-seq, of which 14 were confirmed to be expressed within esophageal glands in this study or by other groups (Huang et al., 2003; Nguyen et al., 2018; Rutter et al., 2014). The limited overlap (34%) in effector candidates mined from RNA-seq and LC-MS/MS is likely due to the stringency of our RNA-seq mining strategy, in which an additional filtration step was taken, and genes still expressed within DGs of adult females, but not upregulated when compared to earlier life stages, were discarded. Because our initial proteomics dataset was established with no filters and consisted of only one replicate, the list of 404 DG effector candidates likely includes false positives; however, 83% of the *Mincs* detected by LC-MS/MS were supported by RNA sequencing and 84% (342 Mincs) were proteins found only in PPN, suggesting the quality of the DG-enriched sample using the method developed in this study is also suitable for proteomics analysis.

385

386

387

388

389

Taken together, we have identified novel candidate *Meloidogyne* effector genes expressed exclusively in the DG of adult females that may have essential roles during later stages of parasitism. This novel repertoire provides a promising source for future studies to elucidate the roles these candidate effector genes play during the later phase

of *M. incognita*-host interactions and, thus, unravel additional components – and the processes they entail – necessary for giant cell maintenance and sustained feeding by adult females.

393

394

395

396

397

398

399

400

401

402

403

404

405

406

407

408

409

410

411

412

390

391

392

#### **MATERIAL AND METHODS**

### **DG** collection and enrichment

M. incognita was cultured on greenhouse eggplant roots (Solanum melongena L.). Four-week-old adult females were individually extracted from the roots and immediately placed in a baked cavity slide containing 200 µL of molecular grade ethanol. Once the female nematode was discernibly dehydrated, an incision was cut in the perineal region and the nematode head was manually cut from the body with a scalpel. Pools of 50 female heads were collected in 1.5 mL microcentrifuge tubes containing 1 mL of 100% ethanol. Afterwards, each tube was submitted to 15 min of bath sonication following 15 min of vortexing at full speed to dislodge the contents inside the heads. Homogenates of nematode female heads were applied to a 70 µm mesh cell strainer (pluriStrainer Mini, Germany) placed on top of a 1.5 mL microcentrifuge tube and centrifuged at 500  $\times g$  for 1 min. The collected flow-through was transferred to a 10 µm mesh cell strainer (pluriStrainer Mini, Germany) placed on top of a new microcentrifuge tube and again centrifuged at 500  $\times$  g for 1 min. The DG-enriched cell fractions were obtained by resuspending the material retained on the 10 µm mesh cell strainer. When necessary, DG observation was performed by staining the unfiltered nematode homogenates in 20 μL of HistoGene stain (Applied Biosystems, USA) for 10 min at room temperature. The staining reaction was stopped by adding 200 µL of 100% ethanol to the cell suspension. Filtration was then carried out as previously described and the DGs resuspended in deionized water and mounted on glass slides. Slides were observed with an Olympus BH-2 microscope (Olympus, USA).

416

417

418

419

420

421

422

423

424

425

426

427

428

429

430

431

415

413

414

#### RNA isolation and validation of DG enrichment

Total RNA was extracted from a DG-enriched sample collected from 500 female heads using PicoPure RNA isolation kit (Applied Byosystems, USA). Prior, we verified that approximately 20% of the adult female heads processed through the pipeline described above displayed fully dislodged esophageal glands cells. Thus, one biological replicate was estimated to be 100 fully dislodged DGs. The 10 µm mesh cell strainer retaining DGs was washed with 100 µL of Extraction Buffer (XB), placed on top of a microcentrifuge tube, and centrifuged at 500  $\times$  g for 1 min. Collected flow-through was used in subsequent RNA isolation steps, following the manufacturer's instructions. RNA quality (RIN > 7) and concentration (average of 3.3  $\mu$ g/mL for DG-enriched samples) were verified using an Agilent 2100 RNA 6000 pico kit (Agilent Technologies, USA). To evaluate relative transcript levels from previously identified DG genes, cDNA was generated from DG total RNA using PrimeScript 1st strand cDNA Synthesis Kit (Takara Bio Inc., Japan). Quantitative real-time PCR (RT-qPCR) was performed on a BioRad CFX96 Real-Time System (Bio-Rad Laboratories, USA) using the manufacturer's

CFX96 Real-Time System (Bio-Rad Laboratories, USA) using the manufacturer's recommended reagents and primers listed in **Supplementary table 3**. Thermocycler conditions were as follows: 2 min at 50°C, 2 min at 95°C, followed by 40 cycles of 95°C for 15 sec and 60°C for 1 min. Cycle threshold (Ct) values of each gene were

normalized against *M. incognita* actin (*MiACTIN*, GenBank accession no. BE225475) transcript levels. Relative gene expression was calculated in Microsoft Excel from the determined Ct (dR) values. Statistical comparisons were performed by one-way analysis of variance (ANOVA) available at GraphPad Prism (9.4.1).

440

441

442

443

444

445

446

447

448

449

450

451

452

453

454

455

456

457

458

436

437

438

439

# Library construction, sequencing, and data analysis

RNA-seg results were obtained from three biological replicates of three experimental groups: pre-parasitic second-stage juveniles (ppJ2), female heads (FH), and DGenriched samples. Total RNA (RIN >6) concentration was normalized to 10 ng for each replicate. cDNA synthesis and amplification were performed using SMART-Seg v4 Ultra Low Input RNA Kit (Takara Bio, USA) following the manufacturer's guidelines. Illuminacompatible libraries were prepared and sequenced by the Georgia Genomics and Bioinformatics Core (GGBC) on a single NextSeq 2000 cell using paired-end (PE) 50 base read length. Trimmomatic v. 0.39 (Bolger et al., 2014) was used to quality trim the raw reads; only surviving PE reads with a minimum length of 30 bases were kept for subsequent downstream mapping. Reads were quality assessed using FastQC software v. 0.11.8 (Andrews, 2011) both before and after trimming. Mapping of the reads to the *M. incognita* v.3 reference genome (available at https://parasite.wormbase.org/Meloidogyne incognita prjeb8714/Info/Index?db=core) was done using STAR aligner v. 2.7 (Dobin et al., 2013) and raw count data were extracted from each sample BAM file using HTSeg software v. 0.9.1 (Anders et al., 2015) for generation of count matrix. Manual filtering was next employed to remove rows whose row sum was ≤ 1 across all samples. The resulting filtered matrix object

460

461

462

463

464

contained 37,160 genes. Differential gene expression analysis was performed using DESeq2 (Love et al., 2014) and edgeR (Robinson et al., 2010) packages. The list of genes in DG-enriched samples were generated by combining the results obtained by both packages. Pair-wise comparisons were done among the three sample groups and genes with a false discovery rate (FDR) ≤ 0.05 were considered statistically differentially expressed.

465

466

467

468

469

470

471

472

473

474

475

476

477

478

479

480

481

### Mining of effector candidates

Prediction of N-terminal signal peptide (SP) and lack of transmembrane domains (TMM) was performed by SignalP v.5.0 (https://services.healthtech.dtu.dk/service.php?SignalP-5.0). Candidates predicted to be secreted were evaluated for any homology shared with proteins from Caenorhabditis elegans by running a local BLASTp at default parameters using BLAST2GO v.5.2.5. Gene ontology annotation was performed using the same tool. Nuclear Localization Signal (NLS) prediction was done by NLStradamus (Nguyen Ba et al., 2009, available at http://www.moseslab.csb.utoronto.ca/NLStradamus/). Further identification of effectorrelated elements was identified by cross referencing our list of genes with a publicly available source list. For the putative cis-regulatory element associated with DG effectors (DOG), we referenced the 457 predicted DG effector protein list provided by Da Rocha and collaborators (2021) at https://doi.org/10.15454/2077EF. For identification of Motif EmeRging and with Classes Identification (MERCI) effectorenriched motifs in the 100 first amino acids, the RKN source list was provided by Grymberg et al. (2020) at https://doi.org/10.15454/LMY6LV.

# In situ hybridization

In situ hybridization was performed as described by De Boer et al. (1998) with slight modifications. Adult females (4 weeks-old) displaying egg sacs were individually dissected from roots and decapitated in a cavity slide containing molecular grade 100% ethanol. Heads were accumulated and later fixed in 2% paraformaldehyde in M9 buffer for 18 h at room temperature. Detection was done by incubating (overnight, at 50 °C) the fixed female heads with at least 50 ng of denatured digoxigenin (DIG)-labeled antisense DNA probes, complementary to the transcript of interest. DIG-labeled sense DNA probes were used as negative controls. Staining was observed by addition of anti-DIG antibody (1:500) conjugated to alkaline phosphatase and its respective substrate to hybridized female heads. Samples were monitored and visualized using an Olympus BH-2 Microscope (Olympus, USA) equipped with a Canon EOS M50 camera.

### **Glycoproteomics**

A single DG-enriched sample obtained as previously described was processed for glycoproteomic analysis as described by Wang et al., (2021) with modifications. The sample was sonicated in urea lysis buffer and further homogenized with 28-gauge needle, following its reduction and alkylation by addition of 5 mM DTT and 11 mM iodoacetamide, respectively. Next, buffer exchange of the lysate was carried out using a 3 kDa MWCO filter and washing with 50 mM ammonium bicarbonate. The desalted sample was then subjected to trypsin digestion, and resulting tryptic peptides were dried in a speed vac concentrator and resuspended in 0.1% formic acid. LC-MS/MS analysis

506

507

508

509

510

511

512

513

514

515

516

517

518

519

520

521

522

523

524

525

526

527

was conducted using a Thermo Fisher Eclipse Orbitrap Tribrid MS coupled with a RSLCnano LC system (Dionex Ultimate 3000). Data was collected using an HCD triggered CID method and analyzed using Byonic software (Bern et al., 2012). **ACKNOWLEDGMENTS** We thank Ben Averitt, Kurk Lance, and Dean Kemp for nematode culture maintenance during the span of this project. We thank Dr. Magdy Alabady and Dr. Walt Lorenz from the Georgia Genomics and Bioinformatics Core (GGBC) at the University of Georgia for RNA-seg and bioinformatics support. LITERATURE CITED Almagro Armenteros, J.J., Tsirigos, K.D., Sønderby, C.K., Petersen, T.N., Winther, O., Brunak, S., von Heijne, G. and Nielsen, H. 2019. SignalP 5.0 improves signal peptide predictions using deep neural networks. Nat. Biotechnol. 37: 420-423. Álvarez-Ortega, S., Brito, J.A. and Subbotin, S. 2019. Multigene phylogeny of root-knot nematodes and molecular characterization of *Meloidogyne nataliei* Golden, Rose & Bird, 1981 (Nematoda: Tylenchida). Sci. Rep. 9: 1-11. Andrews, S. 2010. FastQC: a quality control tool for high throughput sequence data. Available online at: http://www.bioinformatics.babraham.ac.uk/projects/fastqc

528 Anders, S., Pyl, P.T. and Huber, W. 2015. HTSeq—a Python framework to work with 529 high-throughput sequencing data. Bioinformatics. 31:166-169. 530 531 Bagdonaite, I., Malaker, S.A., Polasky, D.A., Riley, N.M., Schjoldager, K., Vakhrushev, 532 S.Y., Halim, A., Aoki-Kinoshita, K.F., Nesvizhskii, A.I., Bertozzi, C.R. and Wandall, H.H. 533 2022. Glycoproteomics. Nat. Rev. Methods Primers. 2: 1-29. 534 535 Bern, M., Kil, Y.J. and Becker, C. 2012. Byonic: advanced peptide and protein 536 identification software. Curr. Protoc. Bioinform. 40: 13-20. 537 538 Blanc-Mathieu, R., Perfus-Barbeoch, L., Aury, J.M., Da Rocha, M., Gouzy, J., Sallet, E., 539 Martin-Jimenez, C., Bailly-Bechet, M., Castagnone-Sereno, P., Flot, J.F. and Kozlowski, 540 D.K. 2017. Hybridization and polyploidy enable genomic plasticity without sex in the 541 most devastating plant-parasitic nematodes. PLoS Genet. 13: e1006777. 542 543 Bolger, A.M., Lohse, M. and Usadel, B. 2014. Trimmomatic: a flexible trimmer for 544 Illumina sequence data. Bioinformatics. 30: 2114-2120. 545 546 Chitwood, D.J. 2003. Research on plant-parasitic nematode biology conducted by the 547 United States Department of Agriculture–Agricultural Research Service. Pest Manag. 548 Sci: Formerly Pesticide Science, 59: 748-753. 549

550 Davis, E.L., Hussey, R.S. and Baum, T.J. 2004. Getting to the roots of parasitism by 551 nematodes. Trends Parasitol. 20: 134-141. 552 553 Davis, E.L., Hussey, R.S., Mitchum, M.G. and Baum, T.J. 2008. Parasitism proteins in 554 nematode-plant interactions. Curr. Opin. Plant Biol. 11: 360-366. 555 556 Danchin, E. 2020. M. incognita proteins specific to plant-parasitic nematodes, 557 Recherche Data Gouv, V1. https://doi.org/10.15454/I9MWRS 558 559 Da Rocha, M., Bournaud, C., Dazenière, J., Thorpe, P., Bailly-Bechet, M., Pellegrin, C., 560 Péré, A., Grynberg, P., Perfus-Barbeoch, L., Eves-van den Akker, S. and Danchin, E.G. 561 2021. Genome expression dynamics reveal the parasitism regulatory landscape of the 562 root-knot nematode Meloidogyne incognita and a promoter motif associated with 563 effector genes. Genes. 12: 771. 564 565 De Boer, J.M., Yan, Y., Smant, G., Davis, E.L. and Baum, T.J. 1998. In-situ 566 hybridization to messenger RNA in *Heterodera glycines*. J. Nematol. 30: 309. 567 568 Ding, X., Shields, J., Allen, R. and Hussey, R.S. 1998. A secretory cellulose-binding 569 protein cDNA cloned from the root-knot nematode (Meloidogyne incognita). Mol. Plant-570 Microbe Interact. 11: 952-959. 571

572 Ding, X., Shields, J., Allen, R. and Hussey, R.S. 2000. Molecular cloning and 573 characterisation of a venom allergen AG5-like cDNA from *Meloidogyne incognita*. Int. J. 574 Parasitol. 30: 77-81. 575 576 Dobin, A., Davis, C.A., Schlesinger, F., Drenkow, J., Zaleski, C., Jha, S., Batut, P., 577 Chaisson, M. and Gingeras, T.R. 2013. STAR: ultrafast universal RNA-seg aligner. 578 Bioinformatics 29: 5-21. 579 580 Escobar, C., Barcala, M., Cabrera, J. and Fenoll, C. 2015. Overview of root-knot 581 nematodes and giant cells. In Adv. Bot. Res. 73: 1-32. Academic Press. 582 583 Espada, M., Eves-van den Akker, S., Maier, T., Vijayapalani, P., Baum, T., Mota, M., 584 Jones, J.T., 2018. STATAWAARS: a promoter motif associated with spatial expression 585 in the major effector-producing tissues of the plant-parasitic nematode *Bursaphelenchus* 586 xylophilus. BMC Gen. 19: 553. 587 588 Gao, B., Allen, R., Maier, T., Davis, E.L., Baum, T.J. and Hussey, R.S. 2001. 589 Identification of putative parasitism genes expressed in the esophageal gland cells of 590 the soybean cyst nematode *Heterodera glycines*. Mol. Plant-Microbe Interact. 14: 1247-591 1254. 592 593 Goode, K. and Mitchum, M.G. 2022. Pattern-triggered immunity against root-knot 594 nematode infection: A minireview. Physiol. Plant. 174: e13680.

595 596 Grynberg, P., Coiti Togawa, R., Dias de Freitas, L., Antonino, J.D., Rancurel, C., Mota 597 do Carmo Costa, M., Grossi-de-Sa, M.F., Miller, R.N., Brasileiro, A.C.M., Messenberg 598 Guimaraes, P. and Danchin, E.G. 2020. Comparative genomics reveals novel target 599 genes towards specific control of plant-parasitic nematodes. Genes 11: 1347. 600 601 Huang, G., Gao, B., Maier, T., Allen, R., Davis, E.L., Baum, T.J. and Hussey, R.S. 2003. 602 A profile of putative parasitism genes expressed in the esophageal gland cells of the 603 root-knot nematode *Meloidogyne incognita*. Mol. Plant-Microbe Interact. 16: 376-381. 604 605 Hunt, D.J. and Handoo, Z.A. 2009. Taxonomy, identification and principal species. 606 Root-knot nematodes. 1: 55-88. 607 608 Hussey, R.S. 1989. Disease-inducing secretions of plant-parasitic nematodes. Annu. 609 Rev. Phytopathol. 27: 123-141. 610 611 Hussey, R.S., Davis, E.L. and Baum, T.J. 2002. Secrets in secretions: genes that 612 control nematode parasitism of plants. Braz. J. Plant Physiol. 14: 183-194. 613 614 Hussey, R.S., Huang, G. and Allen, R. 2011. Microaspiration of esophageal gland cells 615 and cDNA library construction for identifying parasitism genes of plant-parasitic 616 nematodes. In Plant Immunity. 89-107. Humana Press. 617

618 Jaubert, S., Laffaire, J.B., Abad, P. and Rosso, M.N. 2002. A polygalacturonase of 619 animal origin isolated from the root-knot nematode *Meloidogyne incognita*. FEBS Lett. 620 522: 109-112. 621 622 Ji, H., Gheysen, G., Denil, S., Lindsey, K., Topping, J.F., Nahar, K., Haegeman, A., De 623 Vos, W.H., Trooskens, G., Van Criekinge, W. and De Meyer, T. 2013. Transcriptional 624 analysis through RNA sequencing of giant cells induced by *Meloidogyne graminicola* in 625 rice roots. J. Exp. Bot. 64: 3885-3898. 626 627 Jones, J.T., Haegeman, A., Danchin, E.G., Gaur, H.S., Helder, J., Jones, M.G., Kikuchi, 628 T., Manzanilla-López, R., Palomares-Rius, J.E., Wesemael, W.M. and Perry, R.N. 2013. 629 Top 10 plant-parasitic nematodes in molecular plant pathology. Mol. Plant Pathol. 14: 630 946-961. 631 632 Jones, M.G. and Goto, D.B. 2011. Root-knot nematodes and giant cells. In Genomics 633 and molecular genetics of plant-nematode interactions. 83-100. Springer, Dordrecht. 634 635 Lambert, K.N., Allen, K.D. and Sussex, I.M. 1999. Cloning and characterization of an 636 esophageal-gland-specific chorismate mutase from the phytoparasitic nematode 637 Meloidogyne javanica. Mol. Plant-Microbe Interact. 12: 328-336. 638

639 Leelarasamee, N., Zhang, L. and Gleason, C. 2018. The root-knot nematode effector 640 MiPFN3 disrupts plant actin filaments and promotes parasitism. PLoS Pathog. 14: 641 e1006947. 642 643 Lilley, C.J., Magbool, A., Wu, D., Yusup, H.B., Jones, L.M., Birch, P.R., Banfield, M.J., 644 Urwin, P.E. and Eves-van den Akker, S. 2018. Effector gene birth in plant parasitic 645 nematodes: Neofunctionalization of a housekeeping glutathione synthetase gene. PLoS 646 Genet. 14: e1007310. 647 648 Lin, B., Qing, X., Liao, J. and Zhuo, K. 2020. Role of protein glycosylation in host-649 pathogen interaction. Cells 9: 1022. 650 651 Love, M.I., Huber, W. and Anders, S. 2014. Moderated estimation of fold change and 652 dispersion for RNA-seq data with DESeq2. Genome Biol. 15: 1-21. 653 654 Maier, T.R., Hewezi, T., Peng, J. and Baum, T.J. 2013. Isolation of whole esophageal 655 gland cells from plant-parasitic nematodes for transcriptome analyses and effector 656 identification. Mol. Plant-Microbe Interact. 26: 31-35. 657 658 Maier, T.R., Masonbrink, R.E., Vijayapalani, P., Gardner, M., Howland, A.D., Mitchum, 659 M.G. and Baum, T.J. 2021. Esophageal gland RNA-Seq resource of a virulent and 660 avirulent population of the soybean cyst nematode *Heterodera glycines*. Mol. Plant-661 Microbe Interact. 34:1084-1087.

662 663 Mejias, J., Bazin, J., Truong, N.M., Chen, Y., Marteu, N., Bouteiller, N., Sawa, S., 664 Crespi, M., Vaucheret, H., Abad, P. and Favery, B. 2021. The root-knot nematode effector MiEFF18 interacts with the plant core spliceosomal protein SmD1 required for 665 666 giant cell formation. New Phytol. 229: 3408-3423. 667 668 Mitchum, M.G., Hussey, R.S., Baum, T.J., Wang, X., Elling, A.A., Wubben, M. and 669 Davis, E.L. 2013. Nematode effector proteins: an emerging paradigm of parasitism. 670 New Phytol. 199: 879-894. 671 672 Mitchum M.G., Rocha, R.O., Huang, G., Maier, T.R., Baum, T.J., and Hussey, R.S. 673 2023. Genome-guided reanalysis of root-knot nematode Meloidogyne incognita 674 esophageal gland cell-enriched sequence tag libraries: a resource for the discovery of 675 novel effectors. PhytoFront. https://doi.org/10.1094/PHYTOFR-09-22-0099-A. 676 677 Nguyen Ba, A.N., Pogoutse, A., Provart, N. and Moses, A.M. 2009. NLStradamus: a 678 simple Hidden Markov Model for nuclear localization signal prediction. BMC Bioinform. 679 10: 1-11. 680 681 Nguyen, C.N., Perfus-Barbeoch, L., Quentin, M., Zhao, J., Magliano, M., Marteu, N., Da 682 Rocha, M., Nottet, N., Abad, P. and Favery, B. 2018. A root-knot nematode small 683 glycine and cysteine-rich secreted effector, MiSGCR1, is involved in plant parasitism. 684 New Phytol. 217: 687-699.

685 686 Paschinger, K., Yan, S. and Wilson, I.B. 2019. N-glycomic Complexity in Anatomical 687 Simplicity: Caenorhabditis elegans as a Non-model Nematode? Front. Mol. Biosci. 6: 9. 688 689 Qin, X., Xue, B., Tian, H., Fang, C., Yu, J., Chen, C., Xue, Q., Jones, J. and Wang, X. 690 2022. An unconventionally secreted effector from the root knot nematode *Meloidogyne* 691 incognita, Mi-ISC-1, promotes parasitism by disrupting salicylic acid biosynthesis in host 692 plants. Mol. Plant Pathol. 23: 516-529. 693 694 Ramazi, S. and Zahiri, J. 2021. Post-translational modifications in proteins: resources, 695 tools and prediction methods. Database, 2021. 696 697 Rivas, S. and Genin, S. 2011. A plethora of virulence strategies hidden behind nuclear 698 targeting of microbial effectors. Front. Plant Sci. 2: 104. 699 700 Robinson, M.D., McCarthy, D.J. and Smyth, G.K. 2010. edgeR: a Bioconductor package 701 for differential expression analysis of digital gene expression data. Bioinformatics. 26: 702 139-140. 703 704 Rutter, W.B., Hewezi, T., Abubucker, S., Maier, T.R., Huang, G., Mitreva, M., Hussey, 705 R.S. and Baum, T.J. 2014. Mining novel effector proteins from the esophageal gland 706 cells of *Meloidogyne incognita*. Mol. Plant-Microbe Interact. 27: 965-974. 707

708 Van de Wouw, A.P. and Idnurm, A. 2019. Biotechnological potential of engineering 709 pathogen effector proteins for use in plant disease management. Biotechnol. Adv. 37: 710 107387. 711 712 Vens, C., Rosso, M.N. and Danchin, E.G. 2011. Identifying discriminative classification-713 based motifs in biological sequences. Bioinformatics. 27: 1231-1238. 714 715 Vieira, P. and Gleason, G., 2019. Plant-parasitic nematode effectors – insights into their 716 diversity and new tools for their identification. Curr. Opin. Plant Biol. 50: 37-43. 717 718 Vieira, P., Shao, J., Vijayapalani, P., Maier, T.R., Pellegrin, C., Eves-van den Akker, S., 719 Baum, T.J. and Nemchinov, L.G. 2020. A new esophageal gland transcriptome reveals 720 signatures of large scale de novo effector birth in the root lesion nematode *Pratylenchus* 721 penetrans. BMC Genet. 21: 1-16. 722 723 Wang, C., Gao, W., Yan, S., Zhu, X.Q., Suo, X., Liu, X., Gupta, N. and Hu, M. 2021. N-724 glycome and N-glycoproteome of a hematophagous parasitic nematode *Haemonchus*. 725 Comput. Struct. Biotechnol. J. 19: 2486-2496. 726 727 Wang, X., Xue, B., Dai, J., Qin, X., Liu, L., Chi, Y., Jones, J.T. and Li, H. 2018. A novel 728 *Meloidogyne incognita* chorismate mutase effector suppresses plant immunity by 729 manipulating the salicylic acid pathway and functions mainly during the early stages of 730 nematode parasitism. Plant Pathol. 67: 1436-1448.

Wang, X., Liu, Q. and Zhang, B. 2014. Leveraging the complementary nature of RNA-Seg and shotgun proteomics data. Proteomics 14: 2676-2687. Zapalska-Sozoniuk, M., Chrobak, L., Kowalczyk, K. and Kankofer, M. 2019. Is it useful to use several "omics" for obtaining valuable results? Mol. Biol. Rep. 46: 3597-3606. 

Table 1. Summary of newly discovered candidate effector genes expressed within esophageal gland cells and identified from DG-enriched samples by RNA-seq

Gene ID	SP	PPN	MERCI	DOG	NLS	Gene Ontology <sup>a</sup>	Gland Location <sup>b</sup>	Amino Acid Similarity	Expression Cluster (Da Rocha, 2021) <sup>c</sup>
Minc3s00519g13668	+	+	+	+	+	C:nucleosome; F:DNA binding; P:nucleosome assembly	DG*	-	G
Minc3s04520g36458	+	+	+	-	+	C:nucleosome; F:DNA binding; P:nucleosome assembly	DG	99.4% similarity to Minc3s00519g13668	G
Minc3s00083g03997	+	+	-	-	+	-	DG*	-	G
Minc3s00324g10218	+	+	+	+	-	-	DG	74.2% similarity to Minc3s00083g03997	Н
Minc3s01037g20083	+	+	+	+	-	-	DG	74.6% similarity to Minc3s00083g03997	Н
Minc3s00078g03784	+	+	+	+	-	-	DG	74.5% similarity to Minc3s00083g03997	Н
Minc3s00202g07467	+	+	+	-	-	C:integral component of membrane	DG*	-	-
Minc3s01184g21492	+	+	+	-	-	C:integral component of membrane	DG	95.1% similarity to Minc3s00202g07467	G
Minc3s00935g19051	+	+	+	-	+	C:integral component of membrane	DG	95.7% similarity to Minc3s00202g07467	G
Minc3s00188g07130	+	+	+	+	-	-	DG*	-	G
Minc3s00020g01309	+	+	+	+	-	-	DG*	-	Н
Minc3s01550g24644	+	+	+	+	-	F:calcium ion binding; F:calcium- dependent phospholipid binding	DG*	-	Н
Minc3s00338g10498	+	+	+	+	-	C:integral component of membrane	DG*	-	Н
Minc3s01603g25044	+	+	+	+	-	C:integral component of membrane	DG	91.0% similarity to Minc3s00338g10498	Н

Minc3s00180g06933	+	+	-	+	-	-	SvG*	-	Н

- <sup>a</sup> For Gene Ontology (GO), C stands for Cellular Component, F is Molecular Function, and P is Biological Process.
- b For gland location, SvG stands for Subventral Glands and DG is Dorsal Gland.
- <sup>c</sup> Gene clustering groups based on transcript expression level as categorized by Da Rocha et al. 2021.
- \*Confirmation by *in situ* hybridization (**Figure 3**).

FIGURE LEGENDS

Figure 1. Validation of dorsal gland enrichment technique. a) Collected glands following enrichment protocol. Glands were stained with HistoGene staining solution. Arrowheads indicate nucleus location. Scale bar is 20  $\mu$ m. **b-d)** Relative transcript abundance of known *Meloidogyne incognita* esophageal gland secretory proteins (Huang, et al. 2003). Significant differences of the means are denoted by different lowercase letters (one-way ANOVA: **b**,  $F_{3,8}$  = 808.1, P < 0.0001; **c**,  $F_{3,8}$  = 1622, P < 0.0001; **d**,  $F_{3,8}$  = 584.1, P < 0.0001). Expression levels were normalized against *M. incognita Actin* gene expression. Error bars indicate standard deviation. For **b-d**, ppJ2, pre-parasitic second-stage juveniles; WF, Whole Females; FH, Female Heads; DG, Dorsal Gland-enriched; Avg, average.

Figure 2. Overview of RNA-seq analysis and effector-mining pipeline to identify novel dorsal gland effector candidates from *M. incognita* adult females. a)

Experimental design included three sample groups, each one consisting of three biological replicates. Reads were mapped to *Meloidogyne incognita* reference genome available at WormBase. b) Differentially expressed genes (DEG) were identified by pairwise comparison of DG with ppJ2 and FH. Only genes (2,033) common to both comparisons were considered for the next steps. c) Out of those, 461 genes were upregulated in dorsal glands samples and, thus, likely enriched in these cells. Further data mining narrowed down the top candidates based on the presence of predicted signal peptide (SP), lack of transmembrane domains (TMM), and no homology to proteins in the free-living nematode *C. elegans.* d) Categorization of the 83 top effector

candidates based on different features, including DOG box (Da Rocha et al., 2021) and MERCI effector motifs (Grynberg, et al., 2020) within their promoter and encoded protein sequences, respectively. Filled-in black dots (connected by vertical lines) indicate what effector-related features are part of the corresponding gene intersection in the bar chart above. For **d**, SP, Signal Peptide; PPN, Plant-Parasitic Nematode-specific; MERCI, Motif EmeRging and with Classes Identification; DOG, DOG Box; NLS, Nuclear Localization Signal.

Figure 3. Detection of dorsal gland effector candidate transcripts by *in situ* hybridization of *M. incognita* adult females. Examples of previously unidentified genes (Mincs) were confirmed to be expressed specifically within the (a) dorsal or (b) subventral esophageal gland cells using DIG-labeled antisense DNA probes. *In situ* hybridization of two known effector candidates (2E07 and 8H11) is also shown. Sense cDNA was used as a negative control and showed no signs of staining. M, metacorpus; SvG, Subventral Glands; DG, Dorsal Glands. Scale bar is 10 μm.

Supplementary figure 1. Cluster dendrogram based on Manhattan's rank coefficient of rlog-transformed expression data. Samples within groups clustered well together with higher correlation among female heads (FH) and dorsal gland-enriched (DG) groups with pre-parasitic juveniles (PPJ) as a distinct outlier. Height indicates degree of similarity between branch points (the greater the height, the greater the difference).

Supplementary figure 2. Detection of transcripts encoding predicted secreted proteins and localized in different  $\it M.$  incognita adult female tissues. Digoxigenin-labeled antisense DNA was used as a probe, and sense cDNA was used as negative control. M, metacorpus. Scale bar is 10  $\mu m$ .

Supplementary figure 3. Complementary aspects of transcriptome and proteome profiles of dorsal gland samples. a) Comparison of the number of all identified proteins in dorsal gland-enriched samples following transcriptomic and proteomic approaches. b) Schematic outline of glycoproteomics analysis performed to support the expression of potential dorsal gland effector candidates and reveal any glycosylation within their protein sequences. c) Distribution of effector-related features among dorsal gland effector candidates identified by proteomics approaches. d) Comparison of the number of mined effector candidates identified by transcriptomic and proteomic approaches. For c, SP, Signal Peptide; PPN, Plant-Parasitic Nematode-specific; MERCI, Motif EmeRging and with Classes Identification; DOG, DOG Box; NLS, Nuclear Localization Signal.

## **TABLES**

**Table 1.** Summary of newly discovered candidate effector genes expressed within esophageal gland cells and identified from DG-enriched samples by RNA-seq.

**Supplementary table 1.** Summary of effector candidate genes identified from DG-enriched samples by RNA-seq.

Supplementary table 2. Summary of candidate effector genes identified from DG-enriched samples by glycoproteomics.
Supplementary table 3. Primers used in this study.

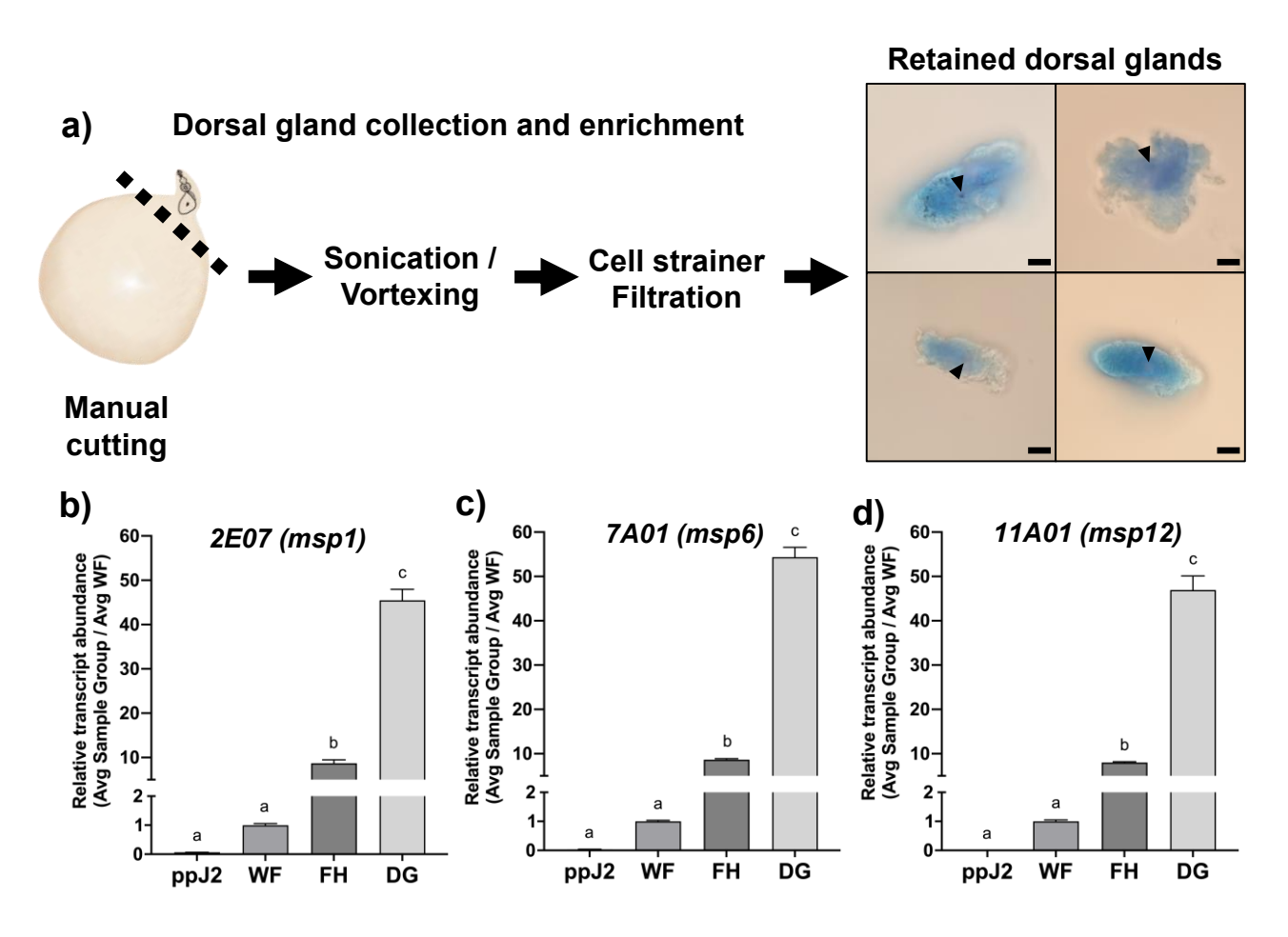
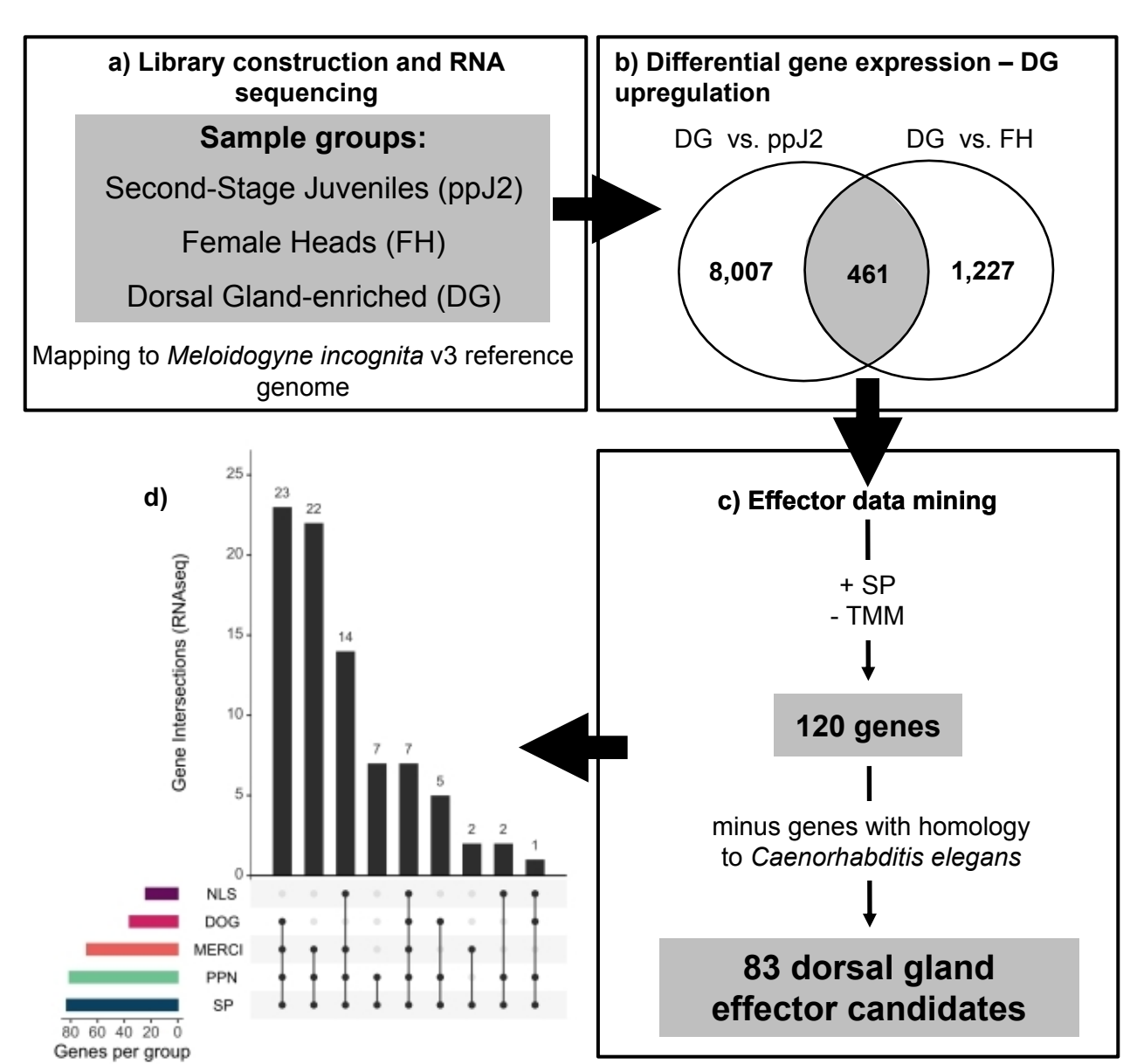


**Figure 1. Validation of dorsal gland enrichment technique. a)** Collected glands following enrichment protocol. Glands were stained with HistoGene staining solution. Arrowheads indicate nucleus location. Scale bar is 20  $\mu$ m. **b-d)** Relative transcript abundance of known *Meloidogyne incognita* esophageal gland secretory proteins (Huang, et al. 2003). Significant differences of the means are denoted by different lowercase letters (one-way ANOVA: **b**,  $F_{3,8} = 808.1$ , P < 0.0001; **c**,  $F_{3,8} = 1622$ , P < 0.0001; **d**,  $F_{3,8} = 584.1$ , P < 0.0001). Expression levels were normalized against *M. incognita Actin* gene expression. Error bars indicate standard deviation. For **b-d**, ppJ2, pre-parasitic second-stage juveniles; WF, Whole Females; FH, Female Heads; DG, Dorsal Gland-enriched; Avg, average.



novel dorsal gland effector candidates from *M. incognita* adult females. a)

Experimental design included three sample groups, each one consisting of three biological replicates. Reads were mapped to *Meloidogyne incognita* reference genome available at WormBase. b) Differentially expressed genes (DEG) were identified by pair-wise comparison of DG with ppJ2 and FH. Only genes (2,033) common to both comparisons were considered for the next steps. c) Out of those, 461 genes were upregulated in dorsal glands samples and, thus, likely enriched in these cells. Further data mining narrowed down the top candidates based on the presence of predicted signal peptide (SP), lack of transmembrane domains (TMM), and no homology to proteins in the free-living nematode *C. elegans.* d) Categorization of the 83 top effector candidates based on different features, including DOG box (Da Rocha et al., 2021) and MERCI effector motifs (Grynberg, et al., 2020) within their promoter and encoded protein sequences, respectively. Filled-in black dots (connected by vertical lines) indicate what effector-related features are part of the

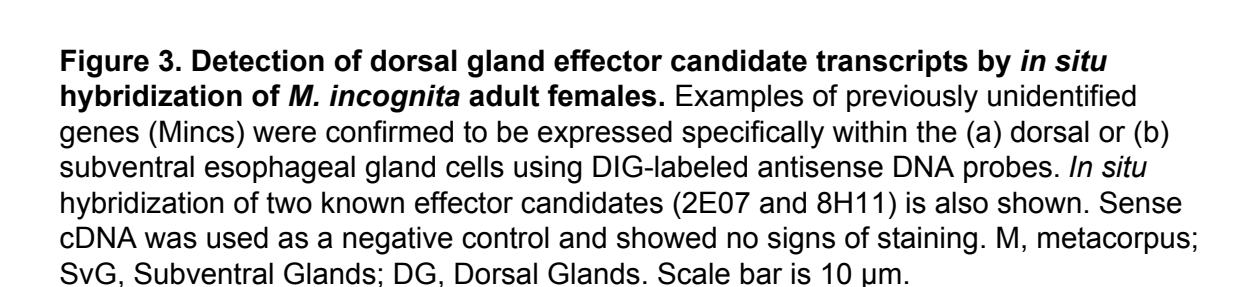
corresponding gene intersection in the bar chart above. For d, SP, Signal Peptide; PPN,

Plant-Parasitic Nematode-specific; MERCI, Motif EmeRging and with Classes

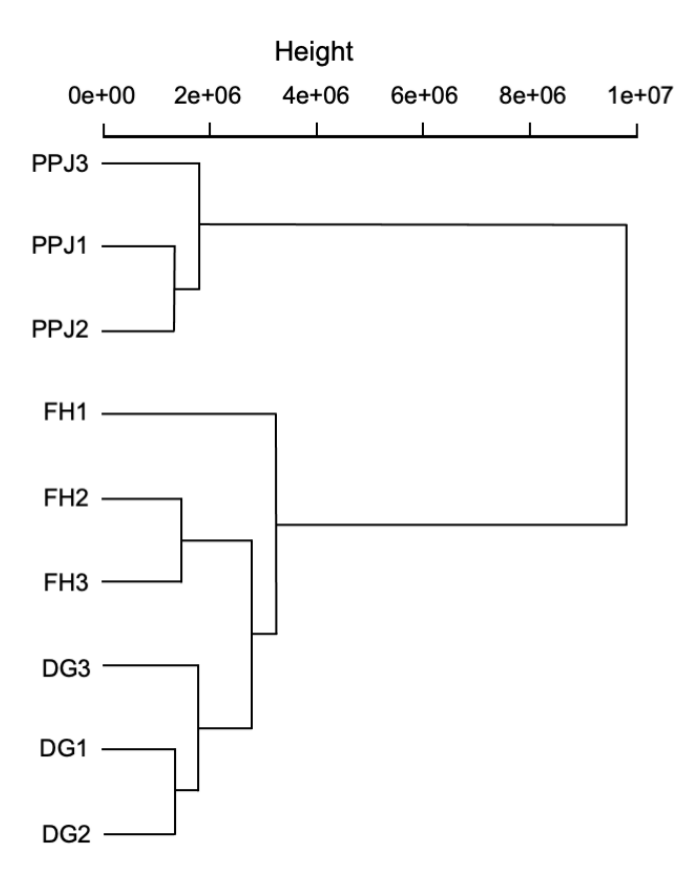
Identification; DOG, DOG Box; NLS, Nuclear Localization Signal.

Figure 2. Overview of RNA-seq analysis and effector-mining pipeline to identify

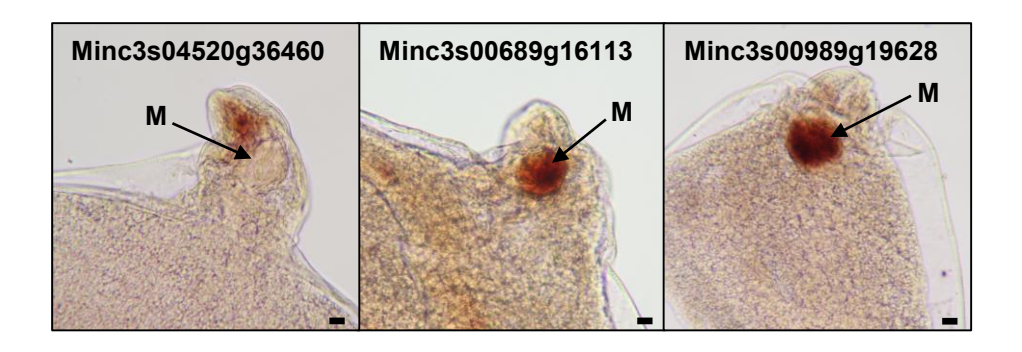
a) Minc3s00173g06738 Minc3s00338g10498 Minc3s00371g11166 (2E07)DG DG Minc3s00519g13668 Minc3s00083g03997 Minc3s00202g07467 DG\_ DG. DG Minc3s00188g07130 Minc3s01550g24644 Minc3s00020g01309 DG b) Minc3s01802g26418 Minc3s05190g37766 Minc3s00180g06933 (8H11) M (30H07 homolog) SvG



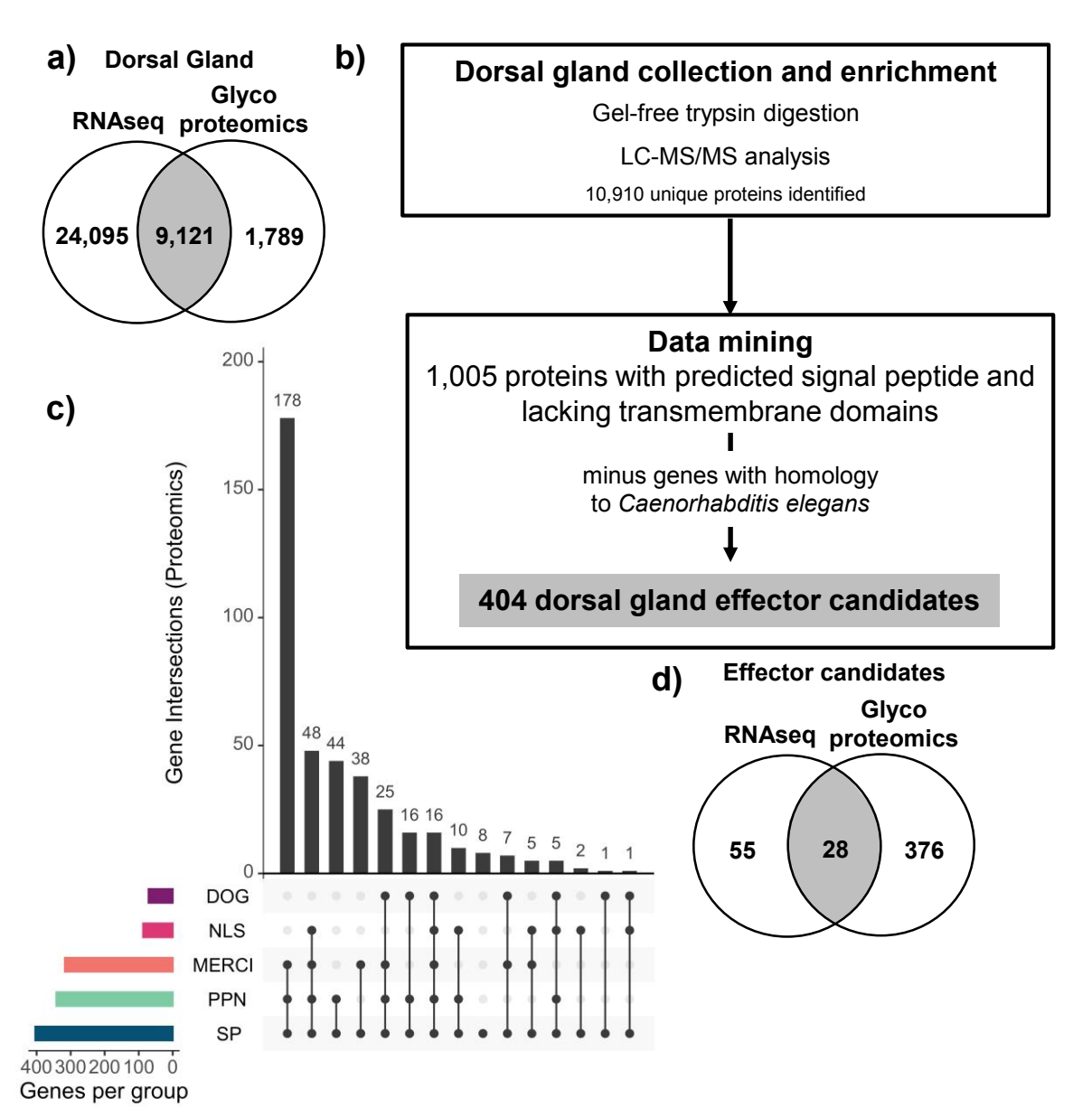
М



Supplementary figure 1. Cluster dendrogram based on Manhattan's rank coefficient of rlog-transformed expression data. Samples within groups clustered well together with higher correlation among female heads (FH) and dorsal gland-enriched (DG) groups with pre-parasitic juveniles (PPJ) as a distinct outlier. Height indicates degree of similarity between branch points (the greater the height, the greater the difference).



Supplementary figure 2. Detection of transcripts encoding predicted secreted proteins and localized in different M. incognita adult female tissues. Digoxigenin-labeled antisense DNA was used as a probe, and sense cDNA was used as negative control. M, metacorpus. Scale bar is 10  $\mu$ m.



Supplementary figure 3. Complementary aspects of transcriptome and proteome profiles of dorsal gland samples. a) Comparison of the number of all identified proteins in dorsal gland-enriched samples following transcriptomic and proteomic approaches. b) Schematic outline of glycoproteomics analysis performed to support the expression of potential dorsal gland effector candidates and reveal any glycosylation within their protein sequences. c) Distribution of effector-related features among dorsal gland effector candidates identified by proteomics approaches. d) Comparison of the number of mined effector candidates identified by transcriptomic and proteomic approaches. For c, SP, Signal Peptide; PPN, Plant-Parasitic Nematode-specific; MERCI, Motif EmeRging and with Classes Identification; DOG, DOG Box; NLS, Nuclear Localization Signal.

## Supplementary table 1. Summary of effector candidate genes identified from DG-enriched samples by RNA-seq.

Gene ID	SP	PPN	MERCI	DOG	NLS	Gene Ontology <sup>a</sup>	in situ <sup>b</sup>	Rediscovered	Reference	Expression Cluster <sup>c</sup>
Minc3s00007g00501	YES	YES					NA			Α
Minc3s00010g00661	YES	YES	YES	YES		C:integral component of membrane; F:protein dimerization activity				G
Minc3s00020g01309	YES	YES	YES	YES			DG			Н
Minc3s00021g01359	YES	YES		YES			NA			G
Minc3s00075g03680	YES	YES	YES			C:membrane; C:integral component of membrane				F
Minc3s00078g03784	YES	YES	YES	YES			DG			Н
Minc3s00083g03997	YES	YES			YES		DG			G
Minc3s00086g04098	YES	YES	YES				NA			
Minc3s00111g04880	YES	YES	YES	YES			DG	11A01	Huang et al., 2003	Н
Minc3s00123g05274	YES	YES	YES	YES			NA			
Minc3s00143g05929	YES	YES	YES		YES					D
Minc3s00144g05949	YES		YES							Α
Minc3s00173g06738	YES	YES	YES	YES			DG	2E07	Huang et al., 2003	Н
Minc3s00173g06739	YES	YES	YES	YES			DG	7A01	Huang et al., 2003	G
Minc3s00180g06933	YES	YES		YES			SvG			Н
Minc3s00184g07017	YES	YES	YES	YES						
Minc3s00188g07130	YES	YES	YES	YES			DG			G
Minc3s00197g07306	YES	YES	YES	YES	YES		NA			G
Minc3s00202g07467	YES	YES	YES			C:integral component of membrane	DG			

						0				
Minc3s00234g08199	YES	YES	YES	YES		C:membrane; C:integral component of membrane	SvG	30H07	Huang et al., 2003	С
Minc3s00237g08283	YES	YES	YES	YES	YES					
Minc3s00249g08563	YES	YES			YES					
Minc3s00251g08591	YES	YES	YES			C:membrane; F:protein dimerization activity				G
Minc3s00266g08975	YES	YES	YES		YES	C:integral component of membrane				
Minc3s00272g09103	YES	YES	YES			JJ				
Minc3s00310g09909	YES	YES	YES	YES	YES		NA			Н
Minc3s00321g10151	YES	YES								G
Minc3s00324g10218	YES	YES	YES	YES			DG			Н
Minc3s00324g10230	YES	YES	YES		YES		NA			G
Minc3s00338g10498	YES	YES	YES	YES		C:integral component of membrane C:membrane;	DG			Н
Minc3s00339g10525	YES	YES	YES		YES	C:integral component of membrane C:membrane;				
Minc3s00353g10813	YES	YES	YES			C:integral component of membrane				F
Minc3s00371g11166	YES	YES		YES			DG	Minc08073	Rutter et al., 2014	Н
Minc3s00389g11471	YES	YES	YES	YES			NA			
Minc3s00477g13005	YES	YES	YES	YES						G
Minc3s00497g13327	YES	YES	YES			C:membrane	SvG	30H07	Huang et al., 2003	С
Minc3s00519g13664	YES	YES	YES		YES	C:nucleosome; F:DNA binding; P:nucleosome assembly	SvG	Minc15401	Rutter et al., 2014	G
Minc3s00519g13668	YES	YES	YES	YES	YES	C:nucleosome; F:DNA binding; P:nucleosome assembly	DG			G

Minc3s00520g13675	YES	YES	YES							
Minc3s00604g14988	YES	YES	YES			F:ATP binding; F:phosphatidylinositol phosphate kinase activity; P:phosphorylation; P:phosphatidylinositol phosphate biosynthetic process				D
Minc3s00624g15265	YES	YES	YES							
Minc3s00689g16113	YES	YES					MC			
Minc3s00815g17702	YES	YES	YES				NA			D
Minc3s00886g18506	YES	YES				C:integral component of membrane				G
Minc3s00897g18643	YES	YES	YES	YES	YES					
Minc3s00935g19051	YES	YES	YES		YES	C:integral component of membrane	DG			G
Minc3s00979g19516	YES	YES	YES				NA			
Minc3s00989g19628	YES	YES	YES				MC			G
Minc3s01014g19856	YES	YES	YES	YES			NA			С
Minc3s01037g20083	YES	YES	YES	YES			DG			Н
Minc3s01142g21139	YES	YES	YES	YES						G
Minc3s01165g21331	YES	YES				C:integral component of membrane				Н
Minc3s01183g21486	YES	YES	YES							
Minc3s01184g21492	YES	YES	YES			C:integral component of membrane	DG			G
Minc3s01198g21633	YES	YES		YES			NA			
Minc3s01208g21728	YES	YES	YES							
Minc3s01226g21877	YES	YES	YES							
Minc3s01525g24488	YES	YES		YES	YES	C:nucleosome; F:DNA binding; P:nucleosome assembly; F:structural	SvG	Minc15401	Rutter et al., 2014	G

						constituent of chromatin				
						F:calcium ion binding;				
Minc3s01550g24644	YES	YES	YES	YES		F:calcium-dependent phospholipid binding	DG			Н
Minc3s01578g24852	YES	YES	YES		YES	-	NA			D
Minc3s01603g25044	YES	YES	YES	YES		C:integral component of membrane	DG			Н
Minc3s01699g25716	YES		YES							
Minc3s01802g26418	YES	YES	YES		YES		SvG	8H11	Huang et al., 2003	G
Minc3s02105g28312	YES	YES	YES		YES		DG	16E05	Huang et al., 2003	
Minc3s02240g29028	YES	YES	YES	YES						
Minc3s02415g29915	YES	YES	YES			C:integral component of membrane	NA			
Minc3s02426g29968	YES	YES	YES	YES		C:integral component of membrane	SvG	30H07	Huang et al., 2003	С
Minc3s02686g31190	YES	YES	YES	YES	YES	C:integral component of membrane				D
Minc3s02734g31393	YES	YES	YES				NA			
Minc3s02982g32304	YES	YES		YES			NA			Α
Minc3s03024g32468	YES	YES	YES	YES			DG	16E05	Huang et al., 2003	
Minc3s03526g34097	YES	YES	YES		YES					
Minc3s03893g35084	YES	YES	YES		YES	C:integral component of membrane C:nucleosome;				
Minc3s04520g36458	YES	YES	YES		YES	F:DNA binding; P:nucleosome assembly	DG			G
Minc3s04520g36460	YES	YES	YES				NA			Н
Minc3s05040g37490	YES	YES	YES					Minc13038	Nguyen et al., 2018	

Minc3s05045g37495	YES	YES	YES	YES			DG	16E05	Huang et al., 2003	
Minc3s05136g37655	YES	YES						Minc13038	Nguyen et al., 2018	G
Minc3s05190g37766	YES	YES	YES			C:integral component of membrane	SvG	30H07	Huang et al., 2003	С
Minc3s05895g38985	YES	YES	YES		YES		SvG	8H11	Huang et al., 2003	G
Minc3s06052g39242	YES	YES	YES	YES	YES	C:nucleosome; F:DNA binding; P:nucleosome assembly	SvG	Minc15401	Rutter et al., 2014	G
Minc3s06349g39698	YES	YES	YES		YES					
Minc3s07416g41097	YES	YES						Minc13038	Nguyen et al., 2018	

<sup>&</sup>lt;sup>a</sup> For Gene Ontology (GO), C stands for Cellular Component, F is Molecular Function, and P is Biological Process. <sup>b</sup> For expression localization by *in situ* hybridization, SvG stands for SubVentral Glands, DG is Dorsal Gland, MC is Metacorpus, and NA is undetermined.

<sup>&</sup>lt;sup>c</sup> Gene clustering groups based on transcript expression level as categorized by Da Rocha et al. 2021.

Supplementary table 2. Summary of effector candidate genes identified from DG-enriched samples by glycoproteomics.

Gene ID	SP	PPN	MERCI	DOG	NLS	Glycosylated
Minc3s00009g00636	YES	YES	YES	YES	YES	
Minc3s00237g08283*	YES	YES	YES	YES	YES	
Minc3s01061g20327	YES	YES	YES	YES	YES	
Minc3s01307g22634	YES	YES	YES	YES	YES	
Minc3s00020g01309*	YES	YES	YES	YES		YES
Minc3s00102g04594	YES	YES	YES	YES		YES
Minc3s01142g21139*	YES	YES	YES	YES		YES
Minc3s00097g04464	YES	YES	YES	YES		
Minc3s00173g06738*	YES	YES	YES	YES		
Minc3s00173g06739*	YES	YES	YES	YES		
Minc3s00188g07130*	YES	YES	YES	YES		
Minc3s00371g11156	YES	YES	YES	YES		
Minc3s00389g11466	YES	YES	YES	YES		
Minc3s00477g13005*	YES	YES	YES	YES		
Minc3s01299g22588	YES	YES	YES	YES		
Minc3s01376g23272	YES	YES	YES	YES		
Minc3s01448g23904	YES	YES	YES	YES		
Minc3s00879g18418	YES	YES	YES		YES	YES
Minc3s00057g02947	YES	YES	YES		YES	YES
Minc3s02354g29629	YES	YES	YES		YES	
Minc3s01210g21747	YES	YES	YES		YES	
Minc3s00067g03380	YES	YES	YES		YES	
Minc3s00116g05066	YES	YES	YES		YES	
Minc3s00143g05929*	YES	YES	YES		YES	
Minc3s00391g11511	YES	YES	YES		YES	

Minc3s00582g14625	YES	YES	YES	YES	
Minc3s01802g26418*	YES	YES	YES	YES	
Minc3s04859g37150	YES	YES	YES	YES	
Minc3s06487g39895	YES	YES	YES	YES	
Minc3s07787g41540	YES	YES	YES		YES
Minc3s00007g00488	YES	YES	YES		YES
Minc3s00009g00581	YES	YES	YES		YES
Minc3s00029g01777	YES	YES	YES		YES
Minc3s00143g05931	YES	YES	YES		YES
Minc3s00292g09561	YES	YES	YES		YES
Minc3s00596g14854	YES	YES	YES		YES
Minc3s01400g23502	YES	YES	YES		YES
Minc3s01755g26079	YES	YES	YES		YES
Minc3s02224g28956	YES	YES	YES		YES
Minc3s03654g34440	YES	YES	YES		YES
Minc3s03801g34858	YES	YES	YES		YES
Minc3s03873g35039	YES	YES	YES		YES
Minc3s05209g37803	YES	YES	YES		YES
Minc3s06165g39437	YES	YES	YES		YES
Minc3s07716g41449	YES	YES	YES		YES
Minc3s01184g21492*	YES	YES	YES		YES
Minc3s01464g24048	YES	YES	YES		YES
Minc3s00014g00910	YES	YES	YES		
Minc3s00044g02436	YES	YES	YES		
Minc3s03594g34270	YES	YES	YES		
Minc3s09540g43307	YES	YES	YES		
Minc3s00007g00484	YES	YES	YES		
Minc3s00007g00493	YES	YES	YES		
Minc3s00014g00947	YES	YES	YES		

Minc3s00020g01290	YES	YES	YES		
Minc3s00021g01355	YES	YES	YES		
Minc3s00033g01963	YES	YES	YES		
Minc3s00058g03008	YES	YES	YES		
Minc3s00071g03524	YES	YES	YES		
Minc3s00076g03726	YES	YES	YES		
Minc3s00097g04444	YES	YES	YES		
Minc3s00100g04535	YES	YES	YES		
Minc3s00100g04543	YES	YES	YES		
Minc3s00118g05113	YES	YES	YES		
Minc3s00132g05599	YES	YES	YES		
Minc3s00142g05905	YES	YES	YES		
Minc3s00159g06378	YES	YES	YES		
Minc3s00159g06381	YES	YES	YES		
Minc3s00161g06429	YES	YES	YES		
Minc3s00172g06704	YES	YES	YES		
Minc3s00213g07676	YES	YES	YES		
Minc3s00218g07824	YES	YES	YES		
Minc3s00218g07844	YES	YES	YES		
Minc3s00249g08565	YES	YES	YES		
Minc3s00272g09116	YES	YES	YES		
Minc3s00282g09338	YES	YES	YES		
Minc3s00295g09620	YES	YES	YES		
Minc3s00299g09671	YES	YES	YES		
Minc3s00351g10780	YES	YES	YES		
Minc3s00492g13235	YES	YES	YES		
Minc3s00523g13719	YES	YES	YES		
Minc3s00558g14270	YES	YES	YES		
Minc3s00688g16089	YES	YES	YES	 	

Minc3s00693g16176	YES	YES	YES	
Minc3s00846g18041	YES	YES	YES	
Minc3s00902g18691	YES	YES	YES	
Minc3s00948g19195	YES	YES	YES	
Minc3s00956g19277	YES	YES	YES	
Minc3s00979g19516*	YES	YES	YES	
Minc3s01017g19897	YES	YES	YES	
Minc3s01035g20064	YES	YES	YES	
Minc3s01113g20842	YES	YES	YES	
Minc3s01124g20947	YES	YES	YES	
Minc3s01321g22758	YES	YES	YES	
Minc3s01432g23766	YES	YES	YES	
Minc3s01518g24443	YES	YES	YES	
Minc3s01616g25126	YES	YES	YES	
Minc3s01620g25147	YES	YES	YES	
Minc3s01642g25285	YES	YES	YES	
Minc3s01686g25595	YES	YES	YES	
Minc3s01763g26124	YES	YES	YES	
Minc3s02399g29853	YES	YES	YES	
Minc3s02658g31083	YES	YES	YES	
Minc3s02713g31296	YES	YES	YES	
Minc3s03150g32958	YES	YES	YES	
Minc3s04145g35601	YES	YES	YES	
Minc3s04270g35901	YES	YES	YES	
Minc3s06413g39792	YES	YES	YES	
Minc3s08913g42748	YES	YES	YES	
Minc3s00523g13708	YES	YES	YES	
Minc3s00976g19489	YES	YES	YES	
Minc3s01077g20499	YES	YES	YES	

Minc3s01309g22654	YES	YES	YES			
Minc3s01527g24496	YES	YES	YES			
Minc3s03265g33333	YES	YES	YES			
Minc3s05178g37747	YES	YES	YES			
Minc3s07353g41022	YES	YES	YES			
Minc3s01478g24139	YES	YES		YES	YES	YES
Minc3s00166g06572	YES	YES		YES	YES	
Minc3s01051g20212	YES	YES		YES		
Minc3s01053g20240	YES	YES		YES		
Minc3s02101g28281	YES	YES		YES		
Minc3s02773g31507	YES	YES		YES		
Minc3s03603g34294	YES	YES		YES		
Minc3s00066g03344	YES	YES			YES	
Minc3s00002g00078	YES	YES				YES
Minc3s00138g05786	YES	YES				YES
Minc3s00282g09343	YES	YES				YES
Minc3s01233g21928	YES	YES				YES
Minc3s01278g22409	YES	YES				YES
Minc3s01172g21396	YES	YES				
Minc3s07231g40879	YES	YES				
Minc3s00648g15590	YES	YES				
Minc3s01319g22740	YES	YES				
Minc3s01412g23601	YES	YES				
Minc3s01535g24536	YES	YES				
Minc3s01844g26697	YES	YES				
Minc3s02847g31794	YES	YES				
Minc3s03156g32976	YES	YES				
Minc3s04173g35665	YES	YES				
Minc3s11461g44907	YES	YES				

Minc3s00226g08023	YES	YES				
Minc3s00383g11372	YES	YES				
Minc3s01470g24092	YES	YES				
Minc3s02512g30400	YES	YES				
Minc3s00716g16467	YES		YES	YES		
Minc3s00181g06936	YES		YES	YES		
Minc3s06138g39396	YES		YES	YES		
Minc3s00330g10330	YES		YES		YES	
Minc3s01454g23943	YES		YES		YES	
Minc3s00026g01673	YES		YES			YES
Minc3s01153g21228	YES		YES			YES
Minc3s05387g38145	YES		YES			YES
Minc3s00518g13645	YES		YES			YES
Minc3s05195g37779	YES		YES			YES
Minc3s00075g03683	YES		YES			
Minc3s00319g10118	YES		YES			
Minc3s00020g01272	YES		YES			
Minc3s00033g01987	YES		YES			
Minc3s00046g02509	YES		YES			
Minc3s00122g05237	YES		YES			
Minc3s00217g07780	YES		YES			
Minc3s00969g19424	YES		YES			
Minc3s01021g19928	YES		YES			
Minc3s02572g30705	YES		YES			
Minc3s02710g31289	YES		YES			
Minc3s03843g34959	YES		YES			
Minc3s00070g03463	YES		YES			
Minc3s00779g17242	YES		YES			
Minc3s00856g18143	YES		YES			

Minc3s03816g34895 YES YES	
Minc3s00022g01422 YES	
Minc3s00069g03420 YES	
Minc3s00679g15987 YES	
Minc3s00199g07377 YES	
Minc3s00225g07997 YES	
Minc3s00197g07306* YES YES YES YES	YES
Minc3s00806g17600 YES YES YES YES	YES
Minc3s00871g18293 YES YES YES YES	YES
Minc3s02686g31190* YES YES YES YES	YES .
Minc3s02720g31334 YES YES YES YES	YES
Minc3s03591g34259 YES YES YES YES	YES
Minc3s00028g01764 YES YES YES YES	YES .
Minc3s00159g06379 YES YES YES YES	YES .
Minc3s00173g06726 YES YES YES YES	YES .
Minc3s00491g13218 YES YES YES YES	/ES
Minc3s00935g19052 YES YES YES YES	/ES
Minc3s01151g21207 YES YES YES YES	/ES
Minc3s00666g15842 YES YES YES YES	YES
Minc3s00010g00661* YES YES YES YES	
Minc3s00035g02089 YES YES YES YES	
Minc3s00043g02402 YES YES YES YES	
Minc3s00221g07893 YES YES YES YES	
Minc3s00234g08199* YES YES YES YES	
Minc3s00519g13667 YES YES YES YES	
Minc3s00610g15098 YES YES YES YES	
Minc3s01037g20083* YES YES YES YES	
Minc3s01550g24644* YES YES YES YES	
Minc3s03024g32468* YES YES YES YES	

 Minc3s05187g37759	YES	YES	YES	YES		
Minc3s00895g18614	YES	YES	YES		YES	YES
Minc3s00057g02946	YES	YES	YES		YES	YES
Minc3s00978g19511	YES	YES	YES		YES	YES
Minc3s05441g38251	YES	YES	YES		YES	YES
Minc3s00026g01665	YES	YES	YES		YES	
Minc3s00323g10215	YES	YES	YES		YES	
Minc3s02248g29071	YES	YES	YES		YES	
Minc3s00020g01295	YES	YES	YES		YES	
Minc3s00083g03979	YES	YES	YES		YES	
Minc3s00197g07312	YES	YES	YES		YES	
Minc3s00272g09105	YES	YES	YES		YES	
Minc3s00315g10024	YES	YES	YES		YES	
Minc3s00324g10230*	YES	YES	YES		YES	
Minc3s00419g12007	YES	YES	YES		YES	
Minc3s00036g02109	YES	YES	YES		YES	
Minc3s00266g08990	YES	YES	YES		YES	
Minc3s00283g09351	YES	YES	YES		YES	
Minc3s00294g09584	YES	YES	YES		YES	
Minc3s00586g14698	YES	YES	YES		YES	
Minc3s01009g19804	YES	YES	YES		YES	
Minc3s01384g23352	YES	YES	YES		YES	
Minc3s03172g33028	YES	YES	YES		YES	
Minc3s00139g05808	YES	YES	YES		YES	
Minc3s00375g11238	YES	YES	YES		YES	
Minc3s00591g14787	YES	YES	YES		YES	
Minc3s00724g16553	YES	YES	YES		YES	
Minc3s01578g24852*	YES	YES	YES		YES	
Minc3s03893g35084*	YES	YES	YES		YES	

	Minc3s06070g39281	YES	YES	YES	YES	
	Minc3s00100g04563	YES	YES	YES	YES	
	Minc3s00106g04722	YES	YES	YES	YES	
	Minc3s00123g05278	YES	YES	YES	YES	
	Minc3s00163g06484	YES	YES	YES	YES	
	Minc3s00586g14705	YES	YES	YES	YES	
	Minc3s00650g15623	YES	YES	YES	YES	
	Minc3s05093g37578	YES	YES	YES	YES	
	Minc3s00020g01299	YES	YES	YES		YES
	Minc3s00037g02167	YES	YES	YES		YES
	Minc3s00058g03000	YES	YES	YES		YES
	Minc3s00604g14988*	YES	YES	YES		YES
	Minc3s00859g18169	YES	YES	YES		YES
	Minc3s01215g21782	YES	YES	YES		YES
	Minc3s01338g22907	YES	YES	YES		YES
	Minc3s01390g23404	YES	YES	YES		YES
	Minc3s01610g25083	YES	YES	YES		YES
	Minc3s00136g05725	YES	YES	YES		YES
	Minc3s00274g09172	YES	YES	YES		YES
	Minc3s00277g09245	YES	YES	YES		YES
	Minc3s01003g19762	YES	YES	YES		YES
	Minc3s02379g29753	YES	YES	YES		YES
	Minc3s03833g34936	YES	YES	YES		YES
	Minc3s04924g37279	YES	YES	YES		YES
	Minc3s00178g06879	YES	YES	YES		
	Minc3s00601g14928	YES	YES	YES		
	Minc3s00030g01829	YES	YES	YES		
	Minc3s00056g02915	YES	YES	YES		
_	Minc3s00058g02987	YES	YES	YES		
	-					

Minc3s00066g03343	YES	YES	YES		
Minc3s00066g03346	YES	YES	YES		
Minc3s00076g03731	YES	YES	YES		
Minc3s00083g03984	YES	YES	YES		
Minc3s00090g04229	YES	YES	YES		
Minc3s00126g05384	YES	YES	YES		
Minc3s00202g07470	YES	YES	YES		
Minc3s00212g07667	YES	YES	YES		
Minc3s00268g09009	YES	YES	YES		
Minc3s00341g10562	YES	YES	YES		
Minc3s00353g10810	YES	YES	YES		
Minc3s00420g12033	YES	YES	YES		
Minc3s00430g12183	YES	YES	YES		
Minc3s00431g12200	YES	YES	YES		
Minc3s00450g12509	YES	YES	YES		
Minc3s00679g15984	YES	YES	YES		
Minc3s00709g16396	YES	YES	YES		
Minc3s00724g16552	YES	YES	YES		
Minc3s00728g16589	YES	YES	YES		
Minc3s00794g17451	YES	YES	YES		
Minc3s01083g20545	YES	YES	YES		
Minc3s01092g20637	YES	YES	YES		
Minc3s01092g20642	YES	YES	YES		
Minc3s01125g20957	YES	YES	YES		
Minc3s01690g25629	YES	YES	YES		
Minc3s01827g26568	YES	YES	YES		
Minc3s02319g29433	YES	YES	YES		
Minc3s02421g29935	YES	YES	YES		
Minc3s02551g30601	YES	YES	YES		

Minc3s02722g31346	YES	YES	YES		
Minc3s03162g32996	YES	YES	YES		
Minc3s03303g33468	YES	YES	YES		
Minc3s03413g33773	YES	YES	YES		
Minc3s03931g35168	YES	YES	YES		
Minc3s04780g36986	YES	YES	YES		
Minc3s04979g37374	YES	YES	YES		
Minc3s05190g37766*	YES	YES	YES		
Minc3s00010g00687	YES	YES	YES		
Minc3s00126g05389	YES	YES	YES		
Minc3s00136g05707	YES	YES	YES		
Minc3s00156g06305	YES	YES	YES		
Minc3s00162g06450	YES	YES	YES		
Minc3s00202g07465	YES	YES	YES		
Minc3s00226g08017	YES	YES	YES		
Minc3s00388g11446	YES	YES	YES		
Minc3s00412g11881	YES	YES	YES		
Minc3s00462g12742	YES	YES	YES		
Minc3s00518g13648	YES	YES	YES		
Minc3s00561g14302	YES	YES	YES		
Minc3s00562g14315	YES	YES	YES		
Minc3s00624g15260	YES	YES	YES		
Minc3s00948g19194	YES	YES	YES		
Minc3s00981g19542	YES	YES	YES		
Minc3s01003g19761	YES	YES	YES		
Minc3s01047g20169	YES	YES	YES		
Minc3s01047g20179	YES	YES	YES		
Minc3s01356g23078	YES	YES	YES		
Minc3s01363g23155	YES	YES	YES		

Minc3s01579g24864	YES	YES	YES			
Minc3s01662g25446	YES	YES	YES			
Minc3s01690g25622	YES	YES	YES			
Minc3s01839g26653	YES	YES	YES			
Minc3s02053g27990	YES	YES	YES			
Minc3s02325g29474	YES	YES	YES			
Minc3s03144g32942	YES	YES	YES			
Minc3s04215g35761	YES	YES	YES			
Minc3s04622g36679	YES	YES	YES			
Minc3s05388g38147	YES	YES	YES			
Minc3s06932g40505	YES	YES	YES			
Minc3s00618g15179	YES	YES		YES	YES	YES
Minc3s00719g16504	YES	YES		YES	YES	
Minc3s01525g24488*	YES	YES		YES	YES	
Minc3s00089g04218	YES	YES		YES		YES
Minc3s00159g06376	YES	YES		YES		
Minc3s00115g05033	YES	YES		YES		
Minc3s00371g11157	YES	YES		YES		
Minc3s00371g11166*	YES	YES		YES		
Minc3s01122g20918	YES	YES		YES		
Minc3s01198g21633*	YES	YES		YES		
Minc3s01331g22845	YES	YES		YES		
Minc3s01703g25740	YES	YES		YES		
Minc3s02982g32304*	YES	YES		YES		
Minc3s08861g42683	YES	YES		YES		
Minc3s00182g06973	YES	YES			YES	YES
Minc3s00748g16837	YES	YES			YES	YES
Minc3s05811g38864	YES	YES			YES	YES
Minc3s00197g07313	YES	YES			YES	

Minc3s00188g07120	YES	YES	YES
Minc3s00275g09183	YES	YES	YES
Minc3s00967g19394	YES	YES	YES
Minc3s00083g03997*	YES	YES	YES
Minc3s00341g10582	YES	YES	YES
Minc3s00110g04854	YES	YES	YES
Minc3s00389g11465	YES	YES	YES
Minc3s01338g22910	YES	YES	YES
Minc3s08890g42721	YES	YES	YES
Minc3s00436g12300	YES	YES	
Minc3s00699g16263	YES	YES	
Minc3s00722g16527	YES	YES	
Minc3s01178g21442	YES	YES	
Minc3s01304g22612	YES	YES	
Minc3s06590g40035	YES	YES	
Minc3s01004g19772	YES	YES	
Minc3s01283g22453	YES	YES	
Minc3s01290g22522	YES	YES	
Minc3s01338g22906	YES	YES	
Minc3s02665g31118	YES	YES	
Minc3s03101g32785	YES	YES	
Minc3s00163g06481	YES	YES	
Minc3s00245g08438	YES	YES	
Minc3s00301g09733	YES	YES	
Minc3s00755g16927	YES	YES	
Minc3s01140g21120	YES	YES	
Minc3s01614g25114	YES	YES	
Minc3s03534g34123	YES	YES	
Minc3s04218g35764	YES	YES	

Minc3s00117g05080	YES	YES	YES		YES
Minc3s00087g04142	YES	YES	YES		
Minc3s00411g11862	YES	YES	YES		
Minc3s00722g16529	YES	YES	YES		
Minc3s00031g01881	YES	YES		YES	YES
Minc3s00919g18882	YES	YES		YES	
Minc3s00139g05823	YES	YES		YES	
Minc3s00339g10517	YES	YES			
Minc3s01180g21464	YES	YES			
Minc3s01898g27040	YES	YES			
Minc3s00007g00448	YES	YES			
Minc3s00230g08131	YES	YES			
Minc3s00272g09117	YES	YES			
Minc3s00453g12571	YES	YES			
Minc3s00490g13205	YES	YES			
Minc3s00746g16803	YES	YES			
Minc3s01081g20527	YES	YES			
Minc3s01917g27183	YES	YES			
Minc3s03425g33806	YES	YES			
Minc3s04771g36974	YES	YES			
Minc3s00132g05610	YES	YES			
Minc3s00856g18140	YES	YES			
Minc3s04159g35628	YES	YES			
Minc3s04932g37290	YES	YES			
Minc3s00636g15427	YES		YES	YES	
Minc3s00066g03329	YES		YES		YES
Minc3s00040g02295	YES			YES	YES
Minc3s02546g30574	YES			YES	
Minc3s04308g36000	YES				
•		· · · · · · · · · · · · · · · · · · ·			

<sup>\*</sup>Effector candidates also identified by transcriptomic approach. *Minc* genes highlighted in gray were identified with Byonic scores greater than 50 and over 5% of the protein sequence covered by peptide-spectrum matches (Bern et al., 2012)

## Supplementary table 3. Primers used in this study.

Gene ID	Primer Purpose	Primer Direction	Sequence	Reference
2E07	qRT-PCR	Forward	GCAATACCTCGGTGGCGTTGGT	Huang <i>et</i> <i>al</i> ., 2003. MPMI
2E07	qRT-PCR	Reverse	CCGCAATCGCCTGAACCTCCTG	Huang <i>et</i> <i>al</i> ., 2003. MPMI
7A01	qRT-PCR	Forward	CCAGCCGAAGTGTGTTGCCCAA	Huang <i>et</i> <i>al</i> ., 2003. MPMI
7A01	qRT-PCR	Reverse	GGGAACGTTGACAGAAGGGCCG	Huang et al., 2003. MPMI
11A01	qRT-PCR	Forward	CCTGTCACTAACATACCATCCG	Xie et al., 2016. Front Plant Sci.
11A01	qRT-PCR	Reverse	GAGGAGGCAAACATTAGG	Xie et al., 2016. Front Plant Sci.
MiACT	qRT-PCR	Forward	GATCCTCACTGAACGTGGTTATTCT	Huang et al. 2006. PNAS
MiACT	qRT-PCR	Reverse	TCCTTGATGTCACGGACATCTC	Huang et al. 2006. PNAS
2E07	<i>in situ</i> hybridization	Forward	ACAAAGTTCAGCAATACCTCGGTGG	
2E07	<i>in situ</i> hybridization	Reverse	CAAGCTGGATGACACACTTGTTGTCG	

11A01	<i>in situ</i> hybridization	Forward	AATAATCGCTATGACCGAGGGTGCA
11A01	<i>in situ</i> hybridization	Reverse	TAACGCCTTATCACCGACAACCAAC
Minc3s00007g00501	<i>in situ</i> hybridization	Forward	ATGAGTGGACAAACCGAGGCTTATG
Minc3s00007g00501	<i>in situ</i> hybridization	Reverse	TCAATTTGGAGATTTTTCTGTTTCTAATCC
Minc3s00020g01309	<i>in situ</i> hybridization	Forward	AAGCGGTGGAGCTAGTCGTGGT
Minc3s00020g01309	<i>in situ</i> hybridization	Reverse	TGCGCGGAAGAGAACATGTCA
Minc3s00083g03997	<i>in situ</i> hybridization	Forward	GAAGGCGTTGAAGCGTGGGACA
Minc3s00083g03997	<i>in situ</i> hybridization	Reverse	TCCTCCAAGGGCATGCTGAAGC
Minc3s00086g04098	<i>in situ</i> hybridization	Forward	CAGCCAGCAGTAGCAAGCGACA
Minc3s00086g04098	<i>in situ</i> hybridization	Reverse	ACCCATAACCACCATAACCGGGGT
Minc3s00123g05274	<i>in situ</i> hybridization	Forward	TCTATCCCCCAATCGGCACACA
Minc3s00123g05274	<i>in situ</i> hybridization	Reverse	AGGCCAAAGTCTTCCACATCGA
Minc3s00180g06933	<i>in situ</i> hybridization	Forward	AAGTTTGCCGTTATGTTCCACG
Minc3s00180g06933	<i>in situ</i> hybridization	Reverse	TCCTTCACGACCGCATATAGGA
Minc3s00188g07130	<i>in situ</i> hybridization	Forward	TGGACTGCAAAATTTCCCCCGA

Minc3s00188g07130	<i>in situ</i> hybridization	Reverse	ACAGCTTCAGCAACCTTGTCCA
Minc3s00197g07306	<i>in situ</i> hybridization	Forward	TGCTCACCGTCATGTATGCCGT
Minc3s00197g07306	<i>in situ</i> hybridization	Reverse	GGCTCCTTTTGGAAGCCTGTCCA
Minc3s00202g07467	<i>in situ</i> hybridization	Forward	GCCTGAGCGCACAATTATATCGT
Minc3s00202g07467	<i>in situ</i> hybridization	Reverse	GCTCTCACTTCCCCAGTGTGCC
Minc3s00310g09909	<i>in situ</i> hybridization	Forward	ACAATTTGTGAAGCCGGGAAGA
Minc3s00310g09909	<i>in situ</i> hybridization	Reverse	TCGCTTCTTTCGGTTCCTCAACA
Minc3s00324g10230	<i>in situ</i> hybridization	Forward	CATGGAGCGGAAGGTACCAGCA
Minc3s00324g10230	<i>in situ</i> hybridization	Reverse	GGGCCTGGGGATTGTGGGGATA
Minc3s00338g10498	<i>in situ</i> hybridization	Forward	TGAGGAACAGCCTTCATCGCCA
Minc3s00338g10498	<i>in situ</i> hybridization	Reverse	TGTGGGAAGTTGCTTTTGGCG
Minc3s00371g11166	<i>in situ</i> hybridization	Forward	ACTCATGCTGAAGCGGACCACC
Minc3s00371g11166	<i>in situ</i> hybridization	Reverse	TGTGTCGCAGCATGATGTGGGG
Minc3s00519g13668	<i>in situ</i> hybridization	Forward	AGCATAAAGCACCTGCTCCCA
Minc3s00519g13668	<i>in situ</i> hybridization	Reverse	TTATTCTTTCCCCCACCCGCGG

Minc3s00689g16113	<i>in situ</i> hybridization	Forward	TGGGTGGATATGGCCAAGCAGGT
Minc3s00689g16113	<i>in situ</i> hybridization	Reverse	AGAATAGCCTCCCTGTCCGG
Minc3s00815g17702	<i>in situ</i> hybridization	Forward	ATGTTATTCATTATCCAATTTACTCTTTTC
Minc3s00815g17702	<i>in situ</i> hybridization	Reverse	TCAAAATAGTGAACAAGATTGCATC
Minc3s00989g19628	<i>in situ</i> hybridization	Forward	TGTATGGCGGGGGAATGAGTGGT
Minc3s00989g19628	<i>in situ</i> hybridization	Reverse	AGGCGGCATAACAGTTTGGCCA
Minc3s01014g19856	<i>in situ</i> hybridization	Forward	TCACAACATTGCTAGAGTTGGGCA
Minc3s01014g19856	<i>in situ</i> hybridization	Reverse	GCATGTTGCGCATTATGCTCCAGC
Minc3s01550g24644	<i>in situ</i> hybridization	Forward	CCTCAATGGCGCCGTGAAGAAA
Minc3s01550g24644	<i>in situ</i> hybridization	Reverse	ACCCAAAGCCTGTTCTCTCGGG
Minc3s01578g24852	<i>in situ</i> hybridization	Forward	TCGTCGTGAATGTTGTGATGAGC
Minc3s01578g24852	<i>in situ</i> hybridization	Reverse	TCCTGCCCATGTTTGTTTCTCCA
Minc3s01802g26418	<i>in situ</i> hybridization	Forward	TGGGGATACTGCTTACAACTGTCC
Minc3s01802g26418	<i>in situ</i> hybridization	Reverse	CATAGTCGGTTGCCACGCCTCT
Minc3s02734g31393	<i>in situ</i> hybridization	Forward	GCAATATGCTGCTGACGGTCAT

Minc3s02734g31393	<i>in situ</i> hybridization	Reverse	TGTTGCCGATCATAGAGATAAGGC	
Minc3s02982g32304	<i>in situ</i> hybridization	Forward	TGTCGTTAGTGTTGCTTGTTGA	
Minc3s02982g32304	<i>in situ</i> hybridization	Reverse	TGTTAGGACATAGCCATATCCAGGT	
Minc3s04520g36460	<i>in situ</i> hybridization	Forward	ACCTAGTTACTCTGAAGGGCCA	
Minc3s04520g36460	<i>in situ</i> hybridization	Reverse	TGTGTAGATCCTCCCCAACCTT	
Minc3s05190g37766	<i>in situ</i> hybridization	Forward	TGGTGAGGAACGTACGCCTACA	
Minc3s05190g37766	<i>in situ</i> hybridization	Reverse	ACAAGGAGGTGTTGGTGCTTCT	